CHALMERS

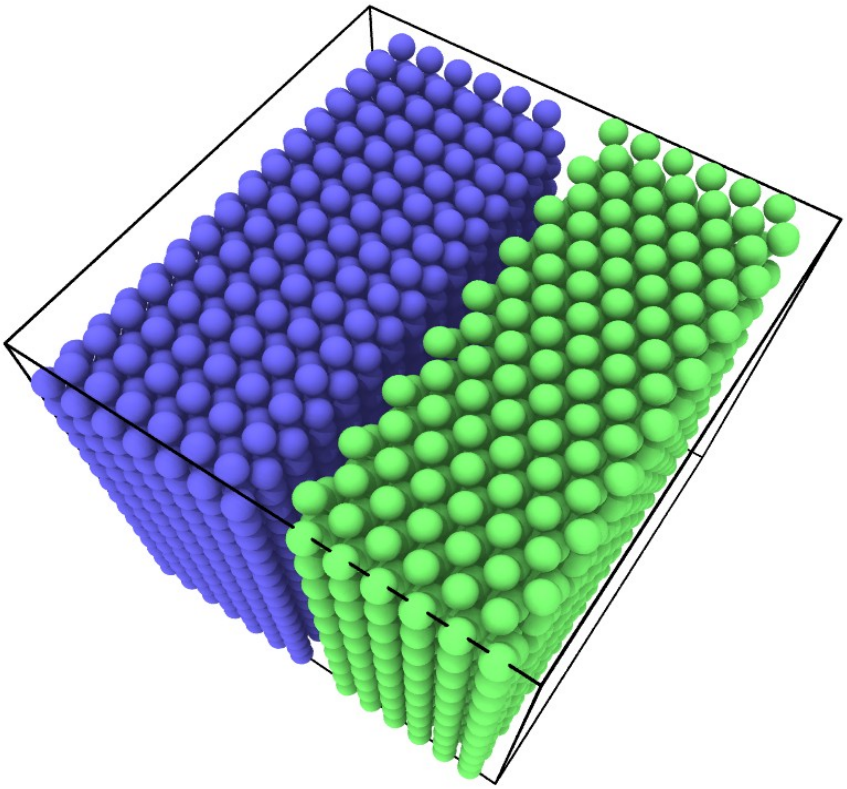

The battle between Energy and Entropy
-Molecular Dynamics and Free Energies

Bachelor's Thesis in Engineering Physics

FREDRIK ERIKSSON
MATTIAS KJELLTOFT
OSKAR LARSSON
MARIKA SVENSSON

Department of Applied Physics
CHALMERS UNIVERSITY OF TECHNOLOGY
Göteborg, Sweden 2014-05-19
Supervisor Paul Erhart

Abstract

The purpose of this report was to illustrate the procedure of calculating a binary phase diagram. In this study, the investigated system was the titanium-tungsten alloy of different compositions at 0 Pa.

The phase diagram of Ti-W alloys is difficult to experimentally determine due to a slow solid-solid transition. To bypass this problem, Molecular Dynamics (MD) simulations were employed using MEAM (Modified Embedded-Atom Method) spline, and CDIP (Composition-Dependent Interatomic Potential) potentials.

Two different simulation methods were used. The direct method simulated a two-phase coexistence of the alloy, which was used to determine the melting lines. For the solid-solid transitions two types of λ-integration were used and compared. These methods are referred to as the multishot and singleshot method in this report.

The direct method was successful and a phase diagram of the high temperature region of the Ti-W alloy was constructed. Issues encountered with the method included a minor energy drift that indicated that the system was not entirely equilibrated as well as difficulties to accurately determine the composition between liquid and solid.

The λ-integration was not so successful. From the beginning the idea was to calculate the phase transitions in the entire solid region but this was abandoned due to time limits. Instead the phase transition for the pure Ti system was calculated and the results compared to the 2012 Master thesis by Tommy Andersson[2]. Unfortunately, his results couldn't be replicated and we suspect some kind of systematic error. However, the ordinary MD-simulations that were run in order to determine the parameters for the λ-integration went well. It showed that a great deal of information can be computed with low effort by ordinary MD-simulations.

To construct the low temperature region of the phase diagram, data provided by Paul Erhart [1], who supervised the project, was used.

Acknowledgements

We would first like to thank Paul Erhart, our supervisor, who with great enthusiasm and effort has guided us. Secondly we would like to thank Chalmers Centre for Computational Science and Engineering (C3SE), provided by the Swedish National Infrastructure for Computing (SNIC), who has provided us with computer resources. Lastly we thank Sandia National Laboratories who provides the open source Molecular Dynamics code LAMMPS.

Contents

Nomenclature

k_b	Bolzmann's constant
bcc	Body centered cubic
c3se	Centre for scientific and technical computing at Chalmers University of Technology in Gothenburg Sweden
CDIP	Composition-dependent interatomic potentials
EAM	Embedded Atom Method
EC	Einstein crystal
GH	Gibbs-Helmholtz
hcp	Hexagonal close packed
LAMMPS	Large-scale Atomic/Molecular Massively Parallel Simulator, an MD-software
MD	Molecular dynamics
MEAM	Modified Embedded Atom Method
NPH	Isoenthalpic-isobaric ensemble
NPT	Isobaric-Isothermal ensemble
NVE	Microcanonical ensemble
NVT	Canonical ensemble
OVITO	Open Visualization Tool, a software for visualizing MD-data
Python	A programming language
TDI	Thermodynamic integration, also called λ-integration
Ti	Titanium
W	Tungsten

Chapter 1

Introduction

In the fields of solid state physics and material sciences it is sometimes difficult to fabricate equilibrated samples of materials at the temperature of solid-solid transitions. This is due their slow transition rates. One example of such a system is tungsten-titanium alloys [3]. This makes it challenging to experimentally determine an accurate low temperature phase diagram.

Since the era of computers began, an alternative way of obtaining phase diagrams has emerged. Through the usage of computer simulations and advanced models of atomic interactions the behavior of these systems are now possible to simulate. These simulations are however computationally very expensive and are preferably performed on large computer clusters. By combining quantum mechanics, experimental results, statistical mechanics and computer sciences these simulations can be performed with good accuracy.

Construction of phase diagrams through atomic simulations are not only theoretically interesting, but it is also useful for calculating properties of the Ti-W alloy when used industrially. W-Ti alloys are for example used in radiation shielding, step soldering and casting [4]. It is also considered to be used in future fusion reactors [5].

1.1 Scope

The purpose of this project was to examine the system of W-Ti and to develop a phase diagram. Research has been conducted in this area before by Lee and Lee 1985 [6], who obtained the phase diagram in figure 1.1. However, their results deviate from reality, especially in the region of low temperature and high ratio of titanium. Ti will undergo transitions between hcp and bcc structures in this region, while W maintain its bcc phase [1]. Our hopes was to be able to get mer accurate results.

In order to complete this task, molecular dynamics simulations were performed. The plan was to simulate with Monte Carlo sampling if time allowed it. This proved not to be the case.

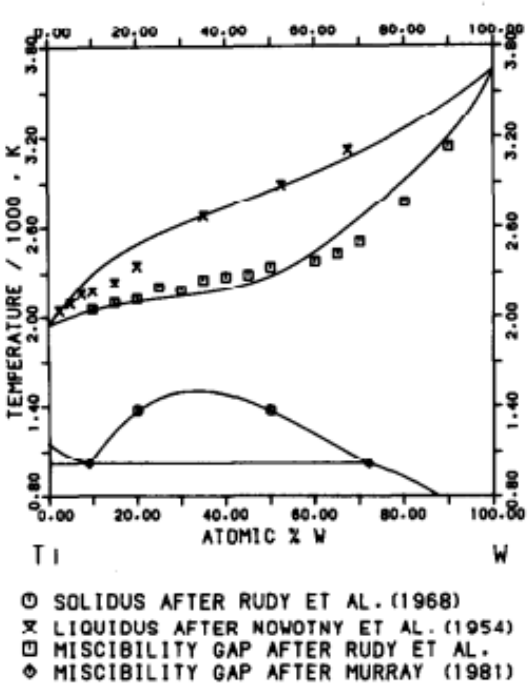

Figure 1.1: Phase diagram of W-Ti alloy computed by Lee and Lee 1985.[6]. Notice the region in the lower left corner with high amount of Ti. This region is thought to deviate from reality and it was one of our goals to properly map out.

Chapter 2

Theory

This section presents the information that is necessary in order to understand the basics of atomic simulations. In section 2.1 a short repetition concerning the basics of thermodynamic and statistical mechanics relevant to this project presented. This is combined with further theory about mixing entropies and energies. In section 2.2 the systems of tungsten and titanium are presented. In the last section about MD-simulations, section 2.3, two different methods utilized in molecular dynamics simulations are introduced.

2.1 Statistical Mechanics and Thermodynamics

The first section provides a short repetition of thermodynamics. The second section, 2.1.2, include theory of sampling thermodynamic properties. In sections 2.1.3 to 2.1.5 Gibbs-Helmholtz formula, phase diagrams and nucleation are presented.

2.1.1 Thermodynamic potentials, ensambles and identities

The behavior of a system of atoms can be explained to some extent by thermodynamics and statistical mechanics. A summary of the basic identities, relations and ensembles concerning this project will be presented below.

The partition function, Z, is derived from the sum of probability of finding an atom in some state s out of all possible states the system has access to. As the system has to be in some state, this is equal to one. This gives rise to

$$1 = \sum_s P(s) = \sum_s \frac{e^{-U(s)/k_B T}}{Z}, \tag{2.1}$$

where $P(s)$ is the probability of the system being in a state s. Solving for the partition function generates the expression

$$Z = \sum_s e^{-U(s)/k_B T}, \tag{2.2}$$

where s is a particular state. The partition function is a fundamental property of a system since other thermodynamic variables can be derived from it. As an example, the average energy can be derived accordingly

$$\bar{U} = \sum_s U(s)P(s) = \frac{1}{Z}\sum_s U(s)e^{-U(s)/k_B T} = \frac{1}{Z}\sum_s U(s)e^{-\beta U(s)} = -\frac{\partial ln(Z)}{\partial \beta} = -k_B T^2 \frac{\partial Z}{\partial T},$$

where $\beta = \frac{-1}{k_B T}$. Further, the heat capacity is defined as

$$C_v = \frac{\partial U}{\partial T}, \tag{2.3}$$

at constant volume. Thus, the heat capacity can then be derived as an expression of Z which gives us

$$C = \frac{1}{K_B T^2}\frac{\partial^2 lnZ}{\partial \beta^2}. \tag{2.4}$$

Further we can calculate the entropy as an expression of the partition function according to

$$S = -k_B \sum_s P(s)ln(P(s)) = \frac{\partial (k_B T lnZ)}{\partial T}. \tag{2.5}$$

The free energies are important thermodynamic potentials, we can derive the expression for Helmholtz free energy F. Helmholtz free energy is defined as $F = U - TS$, in terms of the partition function this expression transforms to

$$F = \bar{U} - TS = -k_B T ln(Z). \tag{2.6}$$

If the free energy of a system is known most thermodynamic properties can be derived. This is why free energy calculations are important.[7]

By using the thermodynamic identity $dU = TdS - pdV + \mu dN$, the thermodynamic identity for Helmholtz energy is obtained, giving us

$$dF = -SdT - pdV + \mu dN. \tag{2.7}$$

The following relations can thus be written

$$\left(\frac{dF}{dT}\right)_{V,N} = -S \qquad \left(\frac{dF}{dV}\right)_{T,N} = p \qquad \left(\frac{dF}{dN}\right)_{T,V} = \mu \tag{2.8}$$

The thermodynamic identity can also be obtained for Gibbs free energy. The definition of Gibbs free energy is $G = H - TS$. Notice that G will reduce to F if p is equal to zero due to that the enthalpy is defined as $H = U + pV$. The thermodynamic identity together with the definition of Gibbs free energy will therefor gives rice to the following expression

$$dG = -SdT + Vdp + \mu N. \tag{2.9}$$

By taking the derivative the following relations can be derived

$$\left(\frac{dG}{dT}\right)_{P,\mu} = -S \quad \left(\frac{dG}{dP}\right)_{T,\mu} = V \quad \left(\frac{dG}{d\mu}\right)_{T,p} = N.[8] \tag{2.10}$$

Ensemble types

Systems can have different ensembles. This means that in a particular ensemble a specific set of thermodynamic variables will remain constant. The ensembles which are used in this report are:

- NPT, which means that the number of particles, pressure and temperature are fixed for the system. Also known as the isothermal-isobaric ensamble.
- NPH which means that the number of particles, pressure and enthalpy are fixed. Also known as the isoenthalpic-isobaric ensamble.
- NVE which means that the number of particles, volume and internal energy is fixed for the system. Also known as the microcanonical ensamble.
- NVT, which means that the number of particles, volume and temperature are fixed for the system. Also known as the canonical ensamle.

[9]

2.1.2 Sampling of Thermodynamic Quantities

A substance consists of a great number of atoms which all have their individual position and momentum, as well as other properties such as electron configuration, nuclear shell excitation etc. The sum of all these individual states for all the atoms in the substance at a fixed moment is called a microstate. Microstates are points in the phase space. A macrostate is a group of microstates which all corresponds to the same average quantities, such as the total energy or temperature of the substance.[9]

Naturally, when performing real experiments, there is no access to the microstates. Instead averages can be measured of the system to determine the macrostate. The opposite is true for simulations, where microstates are known and macrostates will be derived from the microstates. The macrostate are obtained by sampling a

large number of microstates and then average these. It is in principle possible to sample all microstates of a system to get perfect averages, but the astoundingly large number of possible configurations in even a relatively small system deem this impossible. Instead one have to choose how to sample the system. Two common approaches to this is molecular dynamics simulations (MD-simulations) and Monte Carlo simulations (MC-simulations).

The first aspect to consider are which contributions to the number of microstates Ω that are the most important. Combinatorics gives us that

$$\Omega = \Omega_{\text{Positions}}\Omega_{\text{Momenta}}\Omega_{\text{Mixture configurations}}\Omega_{\text{Electronic configurations}}\Omega_{\text{Other}}.$$

That is, the total number of microstates is the product of the number of possible configurations of different properties, provided that they are uncorrelated. Some of these properties have a larger number of possible configurations and will thus give a larger contribution to Ω. The greatest part of Ω is provided by the positions, the momenta and the mixture configurations and we can therefore approximate the number of microstates to

$$\Omega = \Omega_{\text{Positions}}\Omega_{\text{Momenta}}\Omega_{\text{Mixture configurations}}.$$

This is where the MD and MC approaches differ.

A sampling of the positions and momenta can together be seen as a trajectory in the phase space and be summarized in $\Omega_{\text{Vibrations}}$. Such a trajectory can be created by setting up a system at an arbitrary configuration, that is a point in the phase space, and then let the system follow a trajectory through phase space by time integrating the equations of motion. This is the approach of MD.

If the system consist of more than one type of atoms the number of microstates of different mixtures will be $\Omega_{\text{Mixture configurations}} \gg 1$ making sample mixture configurations necessary. The trajectory sampled in the MD approach does only cover a small number of such configurations and thus the sampling should be performed in a different manner to extract this quantity. To sample the $\Omega_{\text{Mixture configurations}}$ part of the microstates MC is a better approach. The method is based on sampling a large number of random points in phase space, rather than points connected in a trajectory.[10]

Since the number of microstates Ω is large and the additive quantities are neat to work with it is convenient to use the logarithm. It is usually presented as

$$S = k_B \ln \Omega = k_B \left[\ln \Omega_{\text{Vibrations}} + \ln \Omega_{\text{Mixture configurations}}\right] = S_{\text{Vibrations}} + S_{\text{Mixture configurations}}$$

that is, the entropy of the system.

Since the purpose of this report is to study the free energy of the solid systems, the entropy and further more the enthalpy of the system should be known.

$$G = H - TS$$

The enthalpy, H, consists of a vibrational contribution and a mixture contribution. However, in this case MD is sufficient to sample both quantities since the contributions emerge from different mechanisms. The entropy is related to the number of possible microstates, but one single microstate itself contains no information about the entropy. The opposite is true for enthalpy and each point in phase space can be assigned a value. This means that it is sufficient to sample a trajectory in phase space to receive the enthalpy of mixing as well as the enthalpy of vibrations.

By performing simulations and sampling using either a combination of MD and MC or other methods for sampling both vibrational and mixture contributions to the entropy all the neccesary information is recieved to get the free energy. It is also possible to replace one of the contributions with an analytical approximation. A common approximation of the entropy of mixing, derived through combinatorics and Stirling's approximation reads:

$$\Delta S_{mix} = -Nk_B \left[x \ln x + (1-x)\ln(1-x)\right]. \tag{2.11}$$

Here N is the number of atoms while x and $(1-x)$ are the proportions of the the two atom types [9].

All in all we sample four quantities to calculate the free energy; H_{vib}, H_{mix}, S_{vib} and S_{mix}. The enthalpy of vibration and mixture, as well as the entropy of vibration can be sampled with MD while the entropy of mixing has to be sampled with MC or approximated with an analytical function.

2.1.3 Gibbs-Helmholtz Formula

Gibbs-Helmholtz formula relates the change in free energy to the change in temperature. By definition

$$G = H - TS \quad \text{and} \quad H = U + pV$$

and the thermodynamic identity gives us

$$\mathrm{d}U = T\mathrm{d}S - p\mathrm{d}V.$$

Combining this leads to

$$\mathrm{d}G = -S\mathrm{d}T - V\mathrm{d}p.$$

For $\mathrm{d}p = 0$ this equals to

$$-S = (\mathrm{d}G/\mathrm{d}T).$$

With this in mind we can write

$$\left(\frac{\mathrm{d}(G/T)}{\mathrm{d}T}\right)_p = \{\text{product rule}\} = T^{-1}\left(\frac{\mathrm{d}G}{\mathrm{d}T}\right)_p + G\frac{\mathrm{d}T^{-1}}{\mathrm{d}T} = \frac{-ST - G}{T^2} = -\frac{H}{T^2}$$

which concludes to

$$\left(\frac{\mathrm{d}(G/T)}{\mathrm{d}T}\right)_p = -\frac{H}{T^2}.$$

This is a useful relation since there is in consequence only need for the free energy of a single point with respect to temperature and dependence on temperature for enthalpy of the system to know the free energy for all temperatures.[11]

2.1.4 Phase Diagrams

Phase diagrams are used to illustrate phase changes. To describe how the composition of a mixture changes during a phase transition a binary phase diagram, see figure 1.1, can be used. In this figure the different phase regions are plotted in a temperature-composition diagram.

By Gibbs phase rule we know that in a binary system the degrees of freedom are equal to the number of phases minus three [7]. This means that a system containing only one phase can change its temperature and composition independently. For systems containing two phases, a change in either the composition or their temperature would affect the other property. This will be shown as lines of allowed composition-temperature values in the phase diagram. A three phase system will only be able to exist for one combination of temperature and composition. This is shown as a point in the phase diagram.

If an equilibrated system is located in a two phase part of the phase diagram, and the temperature and proportions of the mixture is known, it will contain two different compositions of the mixture. The values of the different compositions are found by drawing a horizontal line from the initial point, I, to the nearest phase lines. This will result in two new points, the left point, L, and the right point R. The proportion of each composition can then be determined by the lever rule. To e.g. find the proportion of the composition at L, $I_{comp} - L_{comp}$ is divided by $R_{comp} - L_{comp}$.[7]

2.1.5 Heterogeneous and Homogenous Nucleation

The nucleation process is important to understand in order to simulate the process of melting correctly. The effect nucleation gives rise to is relevant in the transition from a crystallographic (solid) state to a non crystallographic state (liquid) as the transition is delayed by the effect when heating or cooling a system.

At the melting point, a temperature is reached where a liquid and a solid state of an element can coexist. A substance is expected to solidify spontaneously if the temperature is below the melting point due to the difference in Gibbs energy, $\Delta G = G_l - G_s$, which should push the system to undergo a transition. In metals this point is delayed due to nucleation, it is said that a system can be undercooled. The same effect in the oposite direction is called overheating.

There are two types of nucleation, the first type is heterogeneous nucleation which is the effect of a small amount of atoms that are solidified through out the system. This effect however is very small, approximately 1 K.

The other nucleation type is homogeneous nucleation and has a much grater effect, an effect of the order of magnitude 100 K. Homogeneous nucleation occurs when atoms form clusters which are solid in a liquid system. Consider a system which has a cluster of radius r. Gibbs energy for this system is

$$G_1 = V_s G_s + V_l G_l + A_{ls} G_{ls}, \tag{2.12}$$

where V_s, G_s are the volume and Gibbs free energy of the solid. V_l, G_l are the volume and Gibbs free energy of the liquid and A_{ls}, G_{ls} are the area and Gibbs free energy of the interface of liquid and solid. Comparing G_1 to the energy of a pure liquid

$$G_2 = (V_s + V_l)G_l \tag{2.13}$$

The formation free energy of solid can be derived as it is the difference of G_2 and G_1, ie.

$$\Delta G = -V_s(G_l - G_s) + A_{sl}G_{sl}. \tag{2.14}$$

Approximate this type of sequence with clusters to be of spherical shapes with radius r. Equation 2.14 transforms thus to

$$\Delta G = -\frac{4\pi r^3}{3}(G_l - G_s) + 4\pi r^2 G_{sl}, \tag{2.15}$$

which is illustrated in figure 2.1.

In order for the liquid to solidify the maxima of ΔG must be overcome, the maxima is easily obtained by derivation with respect to r to be

$$\Delta G_{maxima} = \frac{16\pi G_{sl}}{3(G_l - G_s)^2} \tag{2.16}$$

at radius

$$r_{maxima} = \frac{2G_{ls}}{(G_l - G_s)}. \tag{2.17}$$

We know further that

$$G_s - G_l = \frac{L\Delta T}{T_m}, \tag{2.18}$$

giving the new expressions

$$\Delta G_{maxima} = \frac{16\pi G_{sl}^3 T_m^2}{3L^2}\frac{1}{\Delta T} \tag{2.19}$$

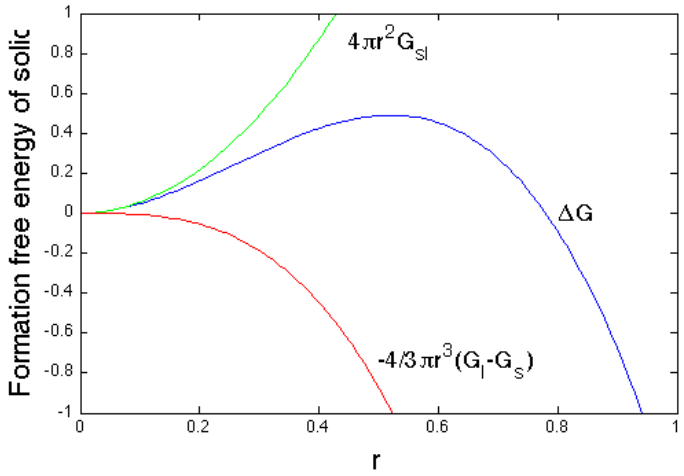

Figure 2.1: Nucleation function for a metal. Even if a state can lower its free energy, (here bulk free energy), by changing to another phase, it still has to overcome a free energy barrier, ΔG^*. This barrier occurs as the free energy increases at the interface between the to phases. However, as the bulk free energy scales with volume and the interface free energy scales with area the total free energy of the system will decrease if a large enough portion transforms.

and

$$r_{maxima} = \frac{2G_{sl}T_m}{L}\frac{1}{\Delta T} \tag{2.20}$$

for the maximum if the radius and Gibbs free energy. Therefor ΔT is the undercooling that is possible before solidification occurs.

Another consequences of nucleation are metastable states. For an equilibrated system, the free energy is minimized. If for a given state for a system, two different phases both corresponds to the lowest possible free energy a phase transition point is reached. At this point both phases are equally likely to exist and the phase of the system will not change as long as the state does not change.

In our case we are looking at Helmholtz free energy. During a phase transition in an equilibrated system the temperature will be constant as the free energy will be constant. If the internal energy of the system were to increase or decrease, the entropy of the system would change in such a way that the free energy would be kept constant.

A system can exist in a state where the free energy is not minimized. This is called a metastable state and these occur due to local minimum in the free energy. One reason for local a minimum is that the energy of the surface tension is added to the total free energy when the phase for a portion of a system changes. This is shown in figure 2.1.[7]

2.2 Elements of Interest

In this report the elements of interest are titanium and tungsten. To get a better understanding of the simulations it is good to have some basic knowledge of the elements that are simulated. The two following sections will be a short overview of the properties of titanium and tungsten.

2.2.1 Titanium

Titanium (Ti) is a transition metal with atomic number 22 that is known for its low density (4.506 g/cm^3 at r.t.) yet high strength. Its strength-to-density ratio is actually the highest of all metallic elements and it is also very resistant to corrosion. The melting point of titanium is 1941 K and it has three different crystalline phases. In this report we will be interested in the solid state transition between hcp and bcc. This occurs at 1155 K. The specific heat raises close to this temperature similarly to what happens at other temperatures of phase transitions.[12]

In the lower right part of the phase diagram in figure 1.1 it is indicated that bcc Ti has higher solubility than hcp Ti in W. The phase diagram for pure titanium is shown in figure 2.3a. Some of the properties of the different phases are discussed below.

α-phase This phase has a hcp structure, see figure 2.2a, and is at atmospheric pressure the equilibrium state of titanium for temperatures below 1155 K [12].

β-phase The β-phase is a bcc structure, see figure 2.2b, and becomes the most stable state at 1155 K [12].

ω-phase This is a hexagonal structure that is only stable at high pressures [12]. It will not be of interest for this report.

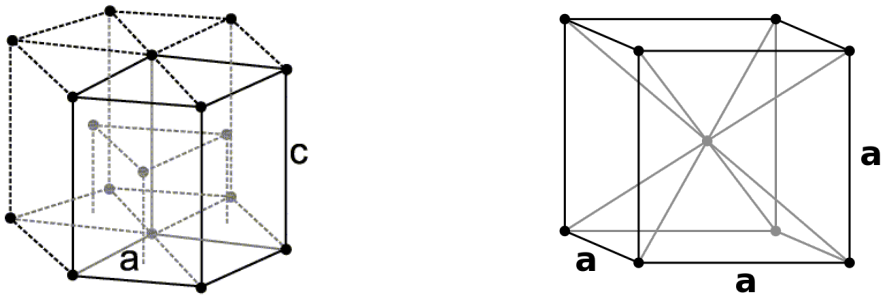

(a) Hcp [13] (b) Bcc [14]

Figure 2.2: The different crystal structures that are of interest for this report. Tungsten is bcc and the crystal structure for Titanium is temperature dependent.

2.2.2 Tungsten

The transition metal tungsten, (W), has atomic number 74. Its distinguishing features are among others high density (19.25 $^{g}/_{cm^3}$ at r.t.), having the highest melting point of all elements (3695 K) as well as being brittle and hard.[15]

It has two crystalline forms referred to as the α and the β. The α-form is the most stable and has a bcc structure, see figure 2.2b; the β-form is only metastable and has a A15 cubic structure. Due to the metastable nature of the A15 cubic form pure tungsten in equilibrium consists of only the bcc structure.[15]

In the lower left part of the phase diagram in figure 1.1 it is indicated that the solubility for W in hcp Ti is close to none. However, above the solid-solid phase transition to bcc Ti the solubility raises. The phase diagram for pure tungsten is shown in figure 2.3b.

2.3 MD Simulations

Since computers became available to researchers simulations have been an important tool for studying interacting systems. A common problem when faced with a computational task is that we know the fundamental equations governing the system, but that these equations only are analytically solvable for a small set of highly idealized problems. For instance the Schrödinger equation in quantum mechanics will give very precise predictions, but it is only analytically solvable for the harmonic oscillator, a particle in a box and the central potential [18]. For any other system approximations and perturbation theory must be applied. By using the simulation approach instead, the problem of unsolvable equations is avoided. Another important application for simulations is that it serves as a complement to experiments due to the simplicity, lower cost and time efficiency.

In this project we are mainly going to use a simulation method called molecular dynamics (MD) in which one assumes that the atoms are point like and therefore can be treated by Newtonian mechanics and then iterates the time forward to compute their trajectories, as described by Frenkel and Smit [10]. The interactions between the atoms are either abstracted from the quantum mechanical, classical mechanical level or measured empirically and implemented in the form of potentials or force fields.

To extract thermodynamic properties from the simulation, the microstates must be sampled. Statistical mechanics is then employed to calculate, for instance, the instantaneous temperature from the average of the particle velocities. The time average of this is then related to the temperature. The whole simulation process closely resembles a real experiment. The simulations in general includes a preparation run of the sample, and a production run. This is when a quantity is measured during a time interval. Statistical noise will be canceled out if the sampling is run long enough.

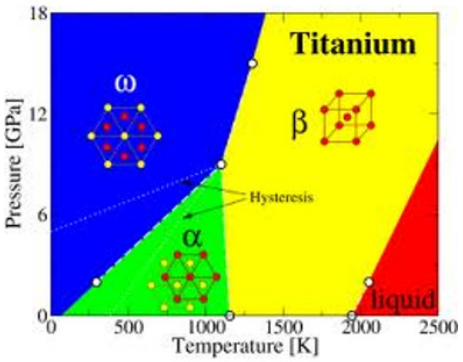

(a) A pressure-temperature phase diagram for pure titanium [16]. The two phases we are interested in are the α (hcp) and the β (bcc).

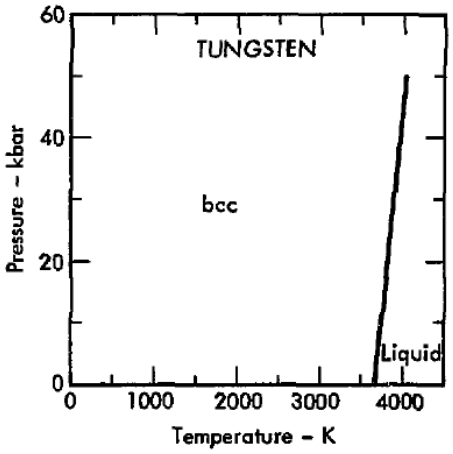

(b) A pressure-temperature phase diagram for pure tungsten [17].

Figure 2.3

2.3.1 Potentials

The type of potentials used in MD simulations are vital to the outcome. There exists many different potentials such as semi-empirical, empirical, embedded etc.. For this project the potentials used were MEAM spline and CDIP potentials.

A MEAM potential is an modified EAM potential. The mathemathical expression for the MEAM potential is

$$E(\bar{\rho}_i, r_{ij}) = \sum_i \left(F_i(\bar{\rho}_i) + \frac{1}{2} \sum_{i \neq j} \phi(r_{ij}) \right). \tag{2.21}$$

The meaning of the MEAM potential is that it computes pairwise forces in addition to what the EAM potential computes. These types of potentials are well suited for for materials of crystal structures sc, bcc, fcc, hcp and diamond.[19]

The CDIP potential us useful for an alloy as it includes the composition dependence, the heat of mixing of the solid solution for the different composition possibilities. [20]

2.3.2 Direct Simulations

When the melting point is the desired point to investigate and determine accurately, the two-phase coexisting simulations with a direct method is a good alternative to λ-integration. This is because theλ-integration can give rice to errors of magnitude of 100 K is not converged correctly. Thus the free energy won't be calculated. As

the name of the direct method indicates, two phases are simulated in direct contact. Direct contact means that there won't exist any barriers between the two phases to separate them.

The desired result of the simulation is to reach a temperature where both solid and liquid phases can exist simultaneously. Consider water and ice as an example, at a temperature below zero o° a system with both water and ice will solidify and become ice and at a temperature above zero the system will liquify. Thus at temperature zero the system will have both liquid water and solid ice in equilibrium.

Employing the direct method for two-phase coexistence simulation, the nucleation will not be a problem because the solid or liquid phase the system can scale the temperature freely. This will make the Gibbs free energies equal for both phases. The correct melting temperature can therefor be achieved. These simulations of two-phase coexisting are stable performed with NPT and NPH ensembles or NPT and NVE ensembles.[21]

It is thus possible to perform NVT and NVE simulations for two-phase coexisting. The problem with employing this method is that it is more difficult to reach the melting point because the energy will be constant. This will easily make the system lose it's two-phase coexisting. [22]

Since a simulation of solid and liquid phases in coexistence requires a large system of at least thousand of atoms in order to get reasonable results, the method will be quite expensive.[21]

The problem for MD simulations is the accuracy of the potentials, specifically MEAM and CDIP potentials used in this report. Interatomic potentials do not guarantee results that recreates experimental values for the non mechanical properties. The non mechanical properties involves the liquid-solid transition. [21]

2.3.3 λ-integration

Thermodynamic integration, the coupling parameter method or λ-integration, is a common and powerful method to calculate the free energy of a system. It was developed by Kirkwood [23] and later implemented in computer simulations by Frenkel and Ladd [24]. λ-integration is a general method and a powerful tool for computation of the free energy although it is computationally somewhat expensive. [2]

Free energy is, unlike temperature and pressure for example, a quantity that can not be derived from the coordinates in phase space. The change in free energy can however be linked to other measurable quantities such as pressure and volume. For example, the change in Helmholtz free energy in an isothermal process is connected to the pressure and volume by

$$\mathrm{d}F = -\mathrm{d}VP.$$

So by choosing a reference system for which there exists an analytical expression for

the total free energy, a thermodynamic path can be selected that takes the reference system to the real system. By monitoring the changes in the thermodynamic quantities the change in free energy can be calculated.

Now consider two systems with internal energies U_A and U_B. By combining these two thermodynamic potentials a path between the two systems by the introduction of a coupling parameter, λ, is created

$$U(\lambda) = U_A + \lambda(U_B - U_A). \tag{2.22}$$

When $\lambda = 0$ the potential energy $U = U_A$ and when $\lambda = 1$ it is $U = U_B$.The for the canonical partition function Z can be expressed as a function of λ accordingly

$$Z(\lambda) = \sum_s \exp(-\beta U_s(\lambda))$$

where $\beta = 1/(k_b T)$. Since Helmholtz free energy F is related to Z , see eq. 2.6, the free energy could be calculated by assuming that the system is in thermodynamic equilibrium and ergodic, i.e. we could replace the ensemble average by a time average.

$$F_B - F_A = \int_0^1 \frac{\mathrm{d}F}{\mathrm{d}\lambda}\,\mathrm{d}\lambda = \int_0^1 \frac{\sum_s (\mathrm{d}U/\mathrm{d}\lambda)\exp(-\beta U_s(\lambda))}{\sum_s \exp(-\beta U_s(\lambda))} = \int_0^1 \left\langle \frac{\mathrm{d}U}{\mathrm{d}\lambda} \right\rangle_\lambda \mathrm{d}\lambda$$

If the coupling function is as in equation (2.22), the calculation of $\langle U_B - U_A \rangle$ can be performed but any function that takes U_A to U_B could in principle be used.

To implement this in a MD simulation the system is equilibrated under the influence of the potential $U(\lambda)$ for different λ values between 0 and 1. For every point in the sampled phase space the energy difference between the two potentials was calculated. The average of this is $\langle U_B - U_A \rangle_\lambda$ for the λ in question.

Since the method only provides the difference in free energy, one of the systems must have a potential for which there exists an analytical expression for the free energy. One such system that is adequate when dealing with solids is the Einstein crystal. The system approximates a solid to have N harmonic oscillators that have no interaction with each other. The free energy can be expressed as

$$\frac{F}{N k_b T} = -\frac{3}{2}\log\left(\frac{k_b^2 T^2 m}{\hbar^2 \alpha}\right).$$

Here m denotes the mass of the particles and α is the spring constant of the oscillators.

For most systems when an Einstein crystal is used as a reference system the difference in internal energies is the same as the difference in potential energies since both systems kinetic energies are the same for a point in phase space, $\langle U_B - U_{Einstein} \rangle_\lambda = \langle E_{pot,B} - E_{pot,Einstein} \rangle_\lambda$.[2]

Chapter 3

Method

To calculate the phase diagram of the alloy the method of molecular dynamics was employed. The most accurate method to solve atomistic and molecular problems is using the Schrödinger equation and from the wave-function calculate the forces on the atoms. Since this is problematic for many-body problems, a simpler and less accurate method exists. By essentially modeling the atoms as point like particles and using a potential to calculate the forces between the atoms, simulating their behavior is possible.[10]

The most important tool was LAMMPS (Large-scale Atomic/Molecular Massively Parallel Simulator), an open source MD software distributed by the US department of energy. LAMMPS integrates Newtons equations of motion for long and short range interaction forces between the particles being simulated. It uses neighbor lists for computational efficiency, in order to exclude computations for atom pairs at a radius where interactions are negligible. When run in parallel it divides the simulation space spatially into several subspaces and assigns one processor to each subspace.[25]

In order to speed up the simulations the code can be run in parallel on many processors. The computation time does not scale perfectly linearly with the number of processors as each processor also keep track of some particles in its neighboring subspaces. This overlap, meaning that multiple processors will keep track of the same particles, will increase with a larger processor to particle ratio. Thus it is better to assign a reasonable number of processors to the simulation for optimal performance, rather than as many as possible. To cut the time of simulations, instead of assigning many processors to work on the same simulation and then perform them sequentially, the simulations can run in parallel.

During the project we had access to a computational cluster called Glenn, which is a Chalmers resource in c3se (Centre for scientific and technical computing at Chalmers University of Technology in Gothenburg Sweden). Glenn has 350 computational nodes with 16 processors and at least 32 GB RAM on each node and is built on AMD Opteron 6220 CPU:s.[26] For our work we used one node per simu-

lation and when we simulated larger datasets we ran several simulations in parallel on separate nodes. This gave us about 30 and 190 atoms per processor for the direct and λ-integration methods respectively. We tried running the λ-integration on two nodes, that is with 15 atoms per processor. This simulation was 22% faster than the one on one node counted in real time and about 50% more expensive in per processor time. We therefore thought that one node was the most reasonable choice.

LAMMPS uses potentials for the implementation of interatomic forces. For the interactions between atoms of the same type we used MEAM spline potentials [19] (W[27], Ti[28]) and for the interactions between W and Ti we used a CDIP potential[29][20].

The post processing of the data was mainly done in python and MATLAB and to some extent OVITO [30].

3.1 Direct Method for Liquid-Solid Transition

The melting region Ti-W alloy that was investigated at a pressure of 0 GPa with MD simulations.

The process of this simulation was to first acquire the hysteresis curve which is the melting interval that nucleation generates. The hysteresis curve was obtained by first simulating the titanium and the tungsten system of 3013 and 3024 atoms respectively from a low initial temperature T_{low} which was chosen considerable much lower than the speculated melting point. The speculated melting point is in this case the experimental values of W and Ti that are 3695 K and 1941 K respectively. The temperature was then ramped to a temperature T_{high} which was about twice the amount of the speculated melting temperatures. The second part of the creation of the hysteresis curve was to simulate the reverse sequence meaning that from a initial high temperature T_{high}, the temperature was decreased to a low temperature T_{low}. For both Ti and W T_{low} was chosen to be 90 K and T_{high} to be 5000 K and 8000 K, respectively.

The simulations for the hysteresis curve in LAMMPS had each one equilibration run of 50 000 steps with 1 fs as the time step in NPT with a Nose-Hoover thermostat. This forced the system to the initial temperature T_{low} or T_{high}, the second part was to ramp up or down the temperature in an additional NPT simulation to T_{low} or T_{high} with the same thermostat and number of steps. A thermostat in LAMMPS is a function that controls the temperature. Due to nucleation the simulation that was ramped up will liquify at a lower temperature than the melting point and the simulation which was ramped down will solidify at a higher temperature than the melting point. An example of the hysteresis curve is shown in figure 3.1 for aluminium.[31]

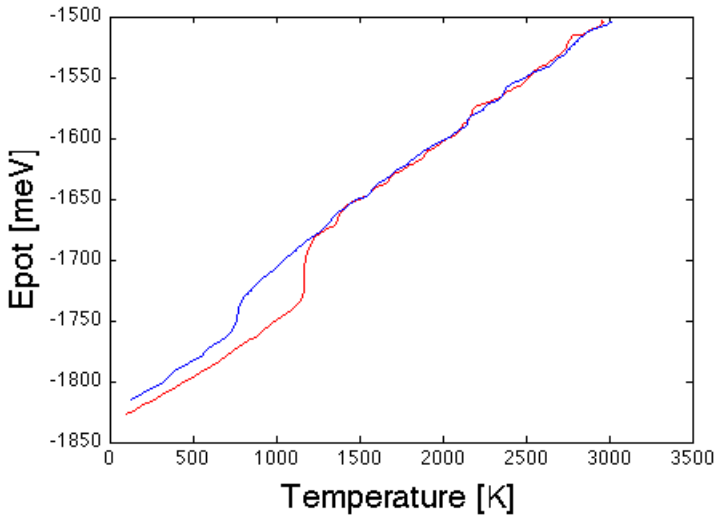

Figure 3.1: The figure shows the melting interval for aluminum

A melting interval for the melting point was now determined. In order to investigate a temperature T_m, which would be a temperature thought to be the melting point, in the melting interval. The direct method for two-phase coexisting simulations were used when simulating the system using LAMMPS.

A time step of 1 fs was used in the simulations with zero pressure for direct method of two-phase simulations. The procedure of the simulation is as follows: the first run is the equilibration run where the entire system was equilibrated to a temperature T_s, which was chosen below but close to the trial melting point T_m, keeping the entire system solid initially. The equilibration run was done in NPT ensemble with 50 000 steps. Then the preparation run is set up where first half the system was melted to a temperature T_{high}, chosen to 8000 K in order to definitely ensure that half the system is melted and not stuck in the melting interval due to nucleation.This was also simulated in an NPT ensemble with 50 000 steps. The solid and the melted half now had an interfacial area at [0,0,1]. The last step in the preparation run was cooling down the melted part of the system to a temperature T_m in NPT ensemble with 50 000 steps. The production run could now begin. The production run was a simulaten in a NPH ensemble where the melted and the solid part were put together again and equilibrated for 400 000 steps.

The procedure of the direct method of two-phase coexisting simulation was iterated with different kinetic energies ie. different T_s and T_m, until the two-phase coexistence was reached for a temperature.

The average temperature from the production run was then calculated and resulted in T_{meltTi}, T_{meltW} and $T^{x_i}_{meltTi-W}$ for different compositions.

Rather than two points being the desired result when simulating the alloy W-Ti for different compositions, the alloy has an entire area to be determined. The alloy

demands more analysis and simulations which are presented in the sections below. The same direct method for two-phase coexisting simulation.

3.1.1 Analyze of the Ti-W alloy

The main problem was to determine the composition of the liquid and solid part for the alloy. The potential energy per atom was dumped by LAMMPS for every 100th step. By taking the average of bin size 20 with respect to time of simulation step between 150 000 to 550 000 production run several plots of the number of atom vs potential energy per atom was generated.

The liquid had a greater potential energy than the liquid, also titanium had a higher potential energy than tungsten. Therefore two Gaussian curves was fitted to the data of titanium and tungsten separately. The functions the data was fitted to was of type

$$f_{tot} = a_1 e^{(-((x-b1)/c1)^2)} + a_2 e^{(-((x-b2)/c2)^2)}. \tag{3.1}$$

The liquid function would be the function which has the higher maximum, so if b1 is grater than b2 the function for the liquid would be

$$f_{liq} = a_1 e^{(-((x-b1)/c1)^2)} \tag{3.2}$$

and the solid function would thus be

$$f_{sol} = a_2 e^{(-((x-b2)/c2)^2)}. \tag{3.3}$$

By integrating the equations, the ratios of liquid Ti and W and solid Ti and W could be determined. Giving the melting lines of the Ti-W alloy by integrating the functions.

3.1.2 Reaching Equilibrium

Due to the fact that the solid part of the alloy couldn't freely change atoms, which was only possible when a vacancy in the solid appeared, a problem to reach equilibrium could be expected. The production run in the direct method was now enhanced to 1 nanosecond, i.e. 10^6 simulation steps to see if there was a difference and to determine is the system was reaching equilibrium. The concentration change was monitored with the software OVTIO.

Also the enthalpy per atom, potential energy per atom and temperature was analyzed to see if the system was evolving to a liquid or a solid state.

If the potential energy was rising while the temperature decreased, the system was for sure evolving to a melted state. The opposite would happen when the potential energy decreased and the temperature was raised.

3.2 λ-integration for Solid-Solid Transition

In order to establish the phase boundaries for the Ti-W alloy in the solid region λ-integration was used. The λ-integration was performed for several different compositions and temperatures for the bcc and hcp phases of the Ti-W alloy. This included pure titanium and pure tungsten.

The simulations gave the free energy F as a function of composition, phase and temperature. Since the phase with the lowest free energy is the most stable, the free energy was used to construct the phase diagram. The construction of the phase diagram is presented in section 3.2.5. The use of λ-integration required a number of parameters that needed to be decided in two separate types of simulations. They are called pre-simulations and will be discussed in section 3.2.1 and 3.2.2. After that the integration step is presented in section 3.2.3. Last, in section 3.2.4, is the use of Gibbs-Helmholtz equation presented. Gibbs-Holmholtz equation is used to interpolate between free energies and to create the actual curve which enable an evaluation of the accuracy of the λ-integration.

3.2.1 Pre-simulations, step 1

First of all we needed good values of the enthalpy over the range of temperatures and compositions for the different phases. This was because we later wanted to use Gibbs-Helmholtz equation to predict the free energy for different temperatures without the need to do expensive λ-integrations. Interpolation and error estimate with GH will be discussed in more detail in section 3.2.4.

From the same simulation it is also possible to extract the volume change due to the change in temperature and composition. This is important since the λ-integration is performed in the NVT ensemble which is very sensitive to volume changes. A high pressure will be induced due to the stress that arises when the volume is changed. This high pressure is because of the, in general high bulk modulus of solids.

This first set of simulations is NPT-simulations with zero pressure. The simulations were performed in cubic systems with around 500 atoms over an interval from 400 K to 1600 K with 100 K steps. This was done for both the hcp and bcc phases for different compositions. The lattice constants for the different phases were set to some value close to the expected. The interval for the compositions was (with pure tungsten as 100%) 2% steps from 0% to 10%, 10% steps from 10% to 80% and then again 2% steps from 80% to 100%. The reason for the larger intervall for the tungsten rich region was because we expected that titanium is much more soluble in tungsten than the other way around.

The simulations was run with a time step of 1 fs. This is a common order of magnitude for these types of simulations and some NVE simulations for Ti were run

and showed no drift in energy. Also, since all simulations are performed in some type of ensemble with constant temperature, the thermostat is able to take care of an eventual drift in energy as long as it's not to large.

The simulations were run for 10 ps in order to be equilibrated. The simulations were then run for 50 ps and the the enthalpy and volume were monitored. The change in volume could then be related to the change in the lattice parameter.

After the first set of pre simulations, the enthalpy and lattice parameter as a function of the composition, phase and temperature was known.

3.2.2 Pre-simulations, step 2

The second set of simulations were performed in order to get a good value for the spring constant that was needed for the λ-integration. In theory we could have used any value but in practice there would have been problems with numeric convergence. As a first guess we used the equation

$$\alpha = 3k_bT/\langle \Delta r^2 \rangle. \tag{3.4}$$

Where α is the spring constant and $\langle \Delta r^2 \rangle$ is the mean square displacement of the system. The meaning of this was to hold the difference between the two systems potential energies as constant as possible. This is because the difference between the potential energies in the EC and the real system is what we wanted to integrate over, in order to get the change in free energy, see section 2.3.3. This is illustrated in figure 4.17.

What was really happening when we chose this particular spring constant were that we used the Einstein model to approximate the density of states for different phonon frequencies to be a delta function. The choosing of the spring constant made sure that the mean frequency was the same for the system and the EC. This is illustrated in figure 3.2. The equation mentioned (3.4) is a rather crude approximation as can be seen in the figure, but it did give a hint about where to start looking for a good value.

When the spring constant was determined, other spring constants close to this value could be tested to see if they made the transition smoother. A smooth and constant function would make the integral converge better.

These second set of simulations were NVT simulations. That is the same ensamble that were used for the λ-integration described later in section 3.2.3. These simulations were run for the same set of compositions as the first pre-simulations described in section 3.2.1. Also, the volume used for different temperatures and compositions was the one that was computed in section 3.2.1. The same time step and equilibration time was used as before but the simulations were run for a shorter time, 30 ps, since the computed spring constant was just a good guess and didn't need to be so converged as the enthalpy or volume in step 1.

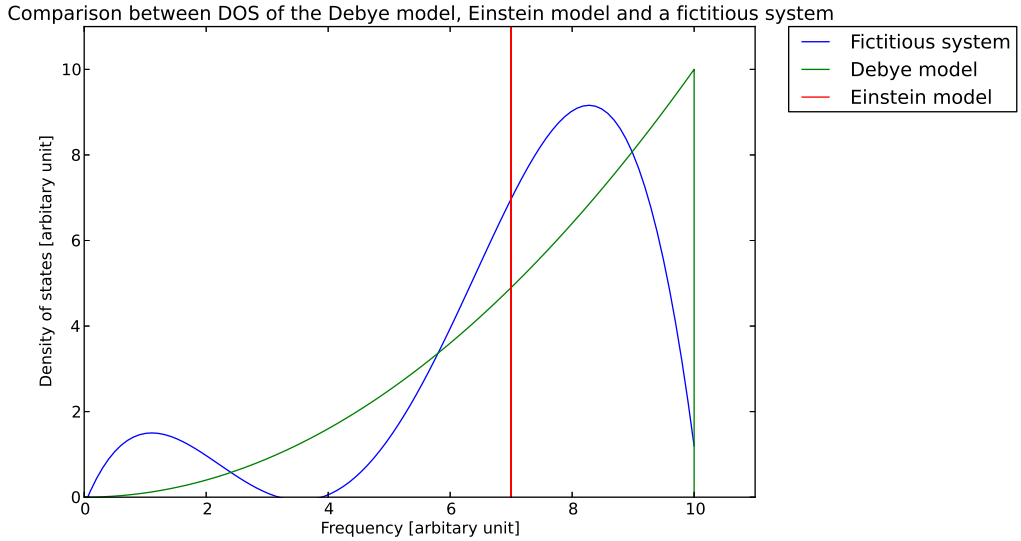

Figure 3.2: This is a comparison between the density of states for different models. The Debye model is better than the Einstein model but the Einstein model is easier to implement in the simulations

The simulations were not run for the same temperatures as the earlier runs since the spring constant is only used for the λ-integration. Thus they were run for the same temperatures that were used in the λ-integrations. Those temperatures were 400 K, 1000 K and 1600 K.

After the second set of pre-simulations were done the spring constant for the different phases, compositions and temperatures was known. After this the λ-integrations could commence.

3.2.3 Integration and convergence

The third step was where the integration was run. When the free energy was calculated it was important to remember that when sampling with MD only the vibrational part of the entropy was taken into account. In order to also make sure that the entropy due to different configurations is included different methods can be used. One such method is Monte Carlo simulations that can be alternated with MD-simulations in order to get a better value for the free energy. We didn't nor couldn't implement such an algorithm efficiently with the current potential so the system entropy was approximated due to different configurations with that of an ideal solution.

The corresponding reference system was still that of an Einstein Crystal but with an extra term that takes the mixing entropy into account according to the following equation

$$\frac{F}{Nk_bT} = -\frac{3}{2}\log\left(\frac{k_b^2T^2m}{\hbar^2\alpha}\right) + (x\log(x) + (1-x)\log(1-x)). \tag{3.5}$$

Two types of λ-integration were tested. The first method will be referred to as the multi-shot method. A number of separate simulations were run for different discrete values of λ. This gave a number of data points for the difference of potential energy between the real system and the EC for each λ. The data points were then integrated over the values of λ from 0 to 1 to get the total free energy difference. The main parameter to get an accurate result is to sample long enough on each value of λ. That is the same as running the simulation for a long enough time. 20 different, evenly spaced λ between 0 and 1 were used. This is a good balance between accuracy and use of computer resources.[2]

The second variant is referred to as the single-shot method. This method was based on the idea that if the system is switched adiabatically it is possible to do the whole integration in one simulation. The advantage was that a much larger set of data points were calculated for different λ. This should in theory increase accuracy. The problem was that when switching the systems, a switch that was to fast won't be adiabatic. Hence it must be done with great care. The main parameter for this method was to switch as slow as possible since a slow switch would increase the number of samples and would hopefully be adiabatic. A simple switch would switch at the same speed over the whole interval. A more delicate method was to make the switch slower at the boundaries (close to $\lambda = 0$ and $\lambda = 1$) where the system would be the least stable. A parametrization of the lambda as a function of a time variable τ according to

$$\lambda(\tau) = \tau^5(70\tau^4 - 315\tau^3 + 540\tau^2 - 420\tau + 126)$$

should have been better.[32]

A good picture to have in mind when thinking about the switch is the following. Imagine that the atoms are interacting with each other with the real potential. Then the switch starts and springs are connected between every atom and the position it vibrates around. Gradually you increase the magnitude of the spring force while the magnitude of the real potential decreases. When the switch is completed, the atoms are moving as if they only were connected by their spring, and the interaction due to the real potential is completely gone.

In order to decide how fast the switching should have been (single-shot) and how long each simulation should have run for each λ (multi-shot) a series of convergence tests were executed. One combination of phase, composition and temperature was used and a number of λ-integrations were run. Different switch times and run times were compared to a very long run of the order of 200 ps to 300 ps. If the calculated free energy differed less than 1 meV the integration was well converged.[2].

In order to decide what spring constant to use a series of simulations were run with different spring constants. They were chosen to be close to the spring constant that was calculated in section 3.2.2. The free energy difference vs. λ was plotted for each run and the spring constant that gave the smoothest function was compared to the guessed spring constant. This step was done for some different compositions,

temperatures and phases in order to see how the spring constant differ from the guessed spring constant.

3.2.4 Interpolating and error estimate with GH

In order to speed up the time for the simulations and to check if the computed values of the free energy were correct, Gibbs-Helmholtz equation was used. This is what the enthalpy was needed for. GH could be used to predict the value of the free energy for different temperatures. This is why only some temperatures were used for the integration. The enthalpy needs to be known for the temperatures between the known value of the free energy and the temperature for the free energy we want to predict. This saved a lot of time since it was easy to calculate enthalpy but hard to calculate the free energy.

The second point was that GH can give an indication about whether the free energy is correct. If the free energy curve predicted with GH doesn't cross the other computed free energy points, something was probably wrong. This is illustrated in figure 3.3. In the figure the GH curve originating from the middle data point differ from the other values with around 10 meV to 100 meV. This would give an indication that the free energy is not so well decided. For example, if the difference between the free energy of the hcp and bcc phases was close or less than 10 meV to 100 meV, not much could have been said about which phase has the lowest free energy.

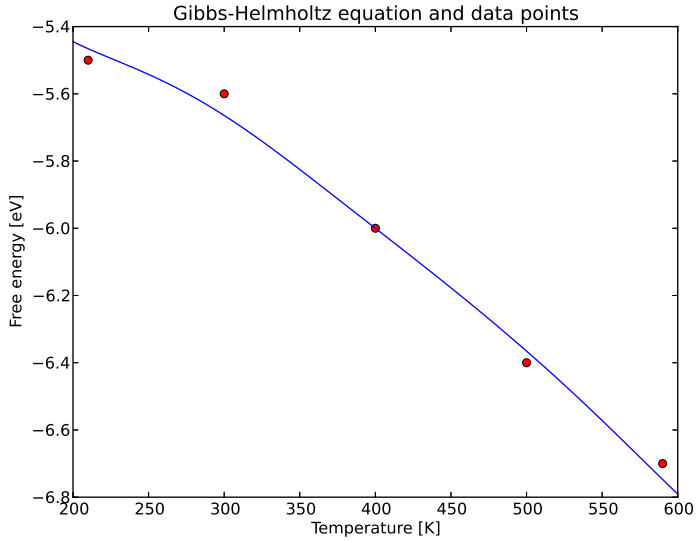

Figure 3.3: This is a graph of the free energy of a fictious solid. The free energy is calculated by Gibbs-Helmholtz equation to temparatures around 400 K. The ideal is that this line would cross inside the data points from the other simulations. From the graph one can see that the error is probably somewhere around 10 meV-100 meV.

3.2.5 Construction of Solid-Solid Phase Diagram

Two different solid-solid binary phase diagrams were created. The first was purely done by approximations and the second was done as a combination of approximations and data. The first step was computing the free energy for systems of different compositions and temperatures.

Then the free energy was plotted in a free energy - composition diagram for different temperatures as seen in figure 3.4. To compute points for the phase diagrams common tangent points in the free energy has to be found. These points can then be plotted in a temperature - composition diagram to create a phase diagram. To numerically check how alike two tangents are the squared area between them were compared.

Pure approxiamtion: The approximations used for construction of this phase diagram was equation 2.11 for the entropy of mixing and the expression in equation 3.6 with $\Omega = 1$ for the enthalpy of mixing. The free energy was then approximated as $\mathrm{H}_{mix} - \mathrm{TS}_{mix}$ as seen in figure 3.4.

$$\mathrm{H}_{mix} = \frac{1}{2}\Omega x(1-x) \tag{3.6}$$

Approximation and data: The H_{mix} data from our own simulations of Ti-W systems was not reliable. For that reason it was provided to us by our supervisor

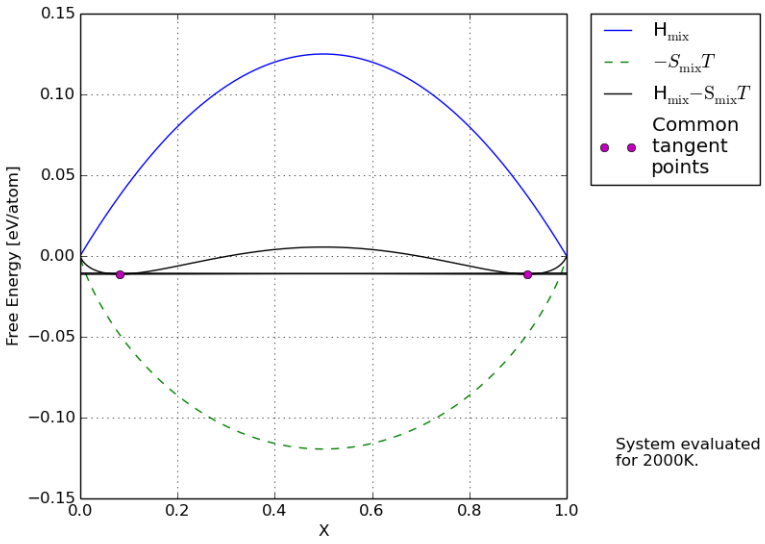

Figure 3.4: Data for constructing phase diagram by using approximations for the enthalpy and entropy of mixing. The purple lines are the common tangents and the purple points the tangent points. A system at this temperature and a composition between the tangent points would get a lower total free energy by dividing it self into two systems of different compositions, each corresponding to one of the common tangent points.

Paul Erhart [1]. H_{mix} is the deviation from a straight line drawn between the total enthalpy of the pure systems.

The fitted curves for the data, as well as the data it self, is shown in figure 3.5. These curves, together with equation 3.6, was used to construct a phase diagram using the same method as for the pure approximation phase diagram.

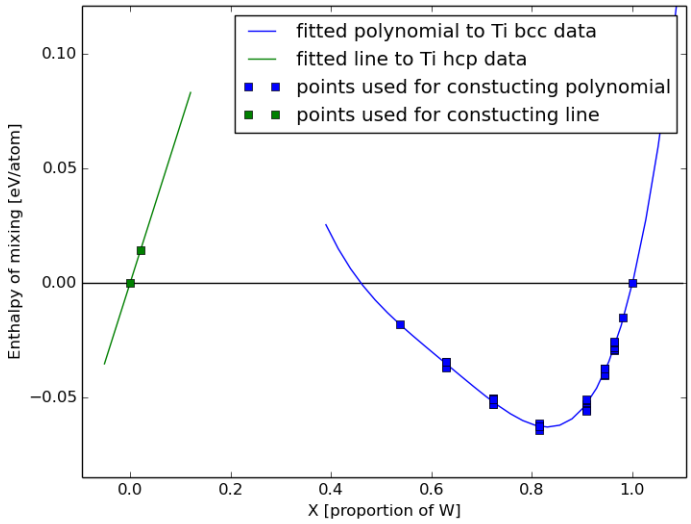

Figure 3.5: Shows how data for H_{mix} from simulations was fitted for further analysis. Note that the polynomial is zero for pure tungsten and the line is zero for pure titanium as there is no enthalpy of mixing for pure substances.

Chapter 4

Result

The complete phase diagram of the Ti-W alloy will be presented in section 4.1. The phase diagram is then broken down in the following sections and the part results are viewed separately. In section 4.2 the results from the two-phase coexisting simulations with the direct method are revealed and in section 4.3 the results of the λ-integration in the solid-solid region will be presented.

4.1 Phase Diagram of Ti-W

The results of the two methods were combined and plotted in a complete phase diagram, which can be seen in figure 4.1. The upper part of the diagram is the melting region, which have been mapped with the direct method in combination with the Gaussian fit method. The lower part of the diagram is the solid-solid two phase region, which have been mapped with common tangent analysis of the data we recieved from our supervisor and should have been mapped with λ-integration.

4.2 Liquid-Solid Transition

The result of the melting lines will be presented in four sections; simulation of the melting interval, pure systems, alloy and last the complete high temperature phase diagram.

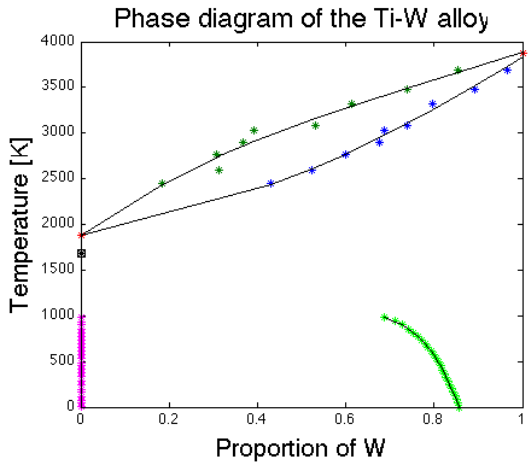

Figure 4.1: The figure shows the results from direct method and λ-integration, ie. the complete phase diagram. The dark green dots and the blue dots represent the boundaries of the two phase melting region, where the dark green dots is representing liquid alloy and the blue dots is representing solid alloy. The two red dots are the melting points of the the pure elements. The pink and light green dots are representing the boundaries of the two phase solid region and the black dot is the computed solid-solid transition point for pure titanium.

4.2.1 Result from hysteresis simulation

From the simulations of the hysteresis the approximative temperature interval of the melting point was determined to [1500,2500] K and [2300,4500] K, which is tabulated in table 4.1 for titanium and tungsten separately.

The simulations are visualized in figure 4.2 and 4.3 with MATLAB for titanium and tungsten, respectively. The blue line in the figures represent the simulation that was equilibrated to a high temperature, 5000 K for Ti and 8000 K for W, and then brought down to a low temperature, 90 K for both Ti and W in LAMMPS. Thus representing a transition from a liquid state to a solid state. The red line is a simulation that was equilibrated to the low temperature and then ramped up to the high temperature, ie. representing a transition form a solid state to a liquid state.

The upper limit, which can be seen in figure 4.2, could clearly be determined for titanium. The lower limit of the melting interval however is less evident due to that titanium is not stable in the lower temperature region, which has a phase transition of second order from solid bcc to solid hcp as the temperature declines.

The upper and lower limit of the melting interval of tungsten could easily be determined as it is stable above and below the melting interval.

Melting interval	T_1	T_2
Titanium	1500 K	2500 K
Tungsten	2300 K	4500 K

Table 4.1: Determined melting interval for Ti and W from the hysteresis simulations

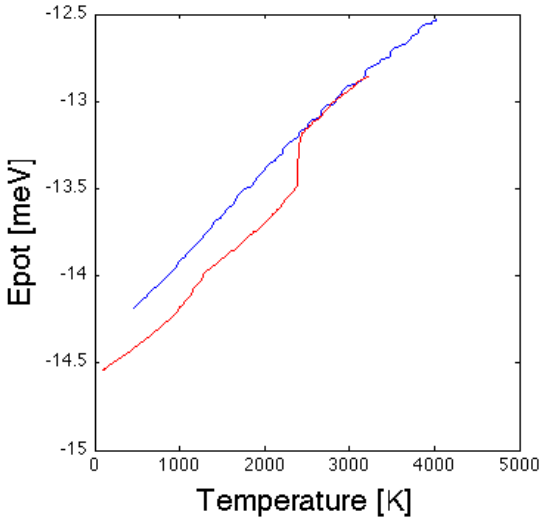

Figure 4.2: Plotted melting interval for titanium from hysteresis simulation in LAMMPS. The blue line symbolizes the transition for Ti from liquid to solid, the red line symbolizes the transition from solid to liquid.

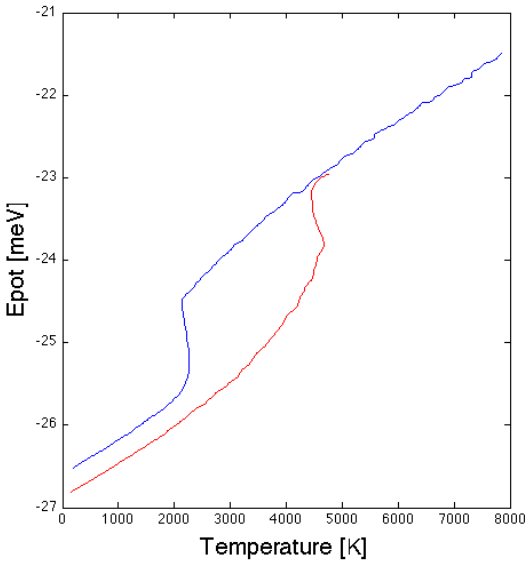

Figure 4.3: Plotted melting interval for tungsten from hysteresis simulation in LAMMPS. The blue line symbolizes the transition for W from liquid to solid, the red line symbolizes the transition from solid to liquid.

4.2.2 Pure Tungsten and Titanium Systems

The direct method for the two-phase coexisting simulation resulted in the melting points of 1883 K and 3884 K for Ti and W, respectively. The standard deviation can be seen in table 4.2.

	T_m	σ(T)
Titanium	1883 K	51 K
Tungsten	3884 K	52 K

Table 4.2: Determined melting points for Ti and W from the two-phase coexisting simulations with a direct method and standard deviation with respect to temperature.

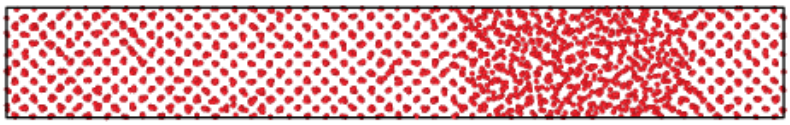

Figure 4.4: Frame 4500 , ie. 450 ps into the simulation, of tungsten in a direct simulation, it can be seen that the liquid and the solid phase both still exist. Therefore the melting point could be reached. The system is visualized in OVITO.

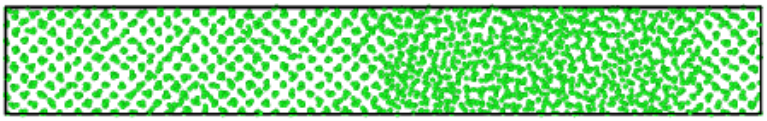

Figure 4.5: Frame 4500, or 450 ps into the simulation, of titanium in a direct simulation. It can be seen that the liquid and the solid phase both still exist. Thus the melting point could be reached. The system is visualized in OVITO.

The two existing phases can clearly be observed in figures 4.4 and 4.5 that are visualized with OVITO for tungsten and titanium. The figures are showing snapshots from the production run in the last time step. Since both phases were still existing when the production run had finished the melting point should be reached.

4.2.3 Melting Lines of Ti-W alloy

The result of the simulation for the alloy at different compositions can be seen in table 4.3 with the standard deviations.

An example of the two phases still coexisting in the simulation of the alloy with 0.5 Ti composition are shown in figure 4.6 at 550 ps into the simulation, these systems are visualized in OVITO. This meant that the temperature of melting should have been reached. In figure 4.7 the two phases still exists after 1 ns. It can be noted that the difference in the amount of liquid has not changed.

W proportion	T_m	solid W proportion	liquid W proportion	σ(T)
0.3	2451 K	0.1838	0.4312	37 K
0.5	2590 K	0.2092	0.3514	57 K
0.45	2765 K	0.3084	0.5984	49 K
0.4	2901 K	0.3151	0.5789	52 K
0.55	3026 K	0.3927	0.6863	57 K
0.6	3086 K	0.4014	0.6229	60 K
0.7	3315 K	0.5213	0.6769	64 K
0.8	3473 K	0.6524	0.8059	61 K
0.9	3684 K	0.8527	0.9660	55 K

Table 4.3: Determined liquid and solid compositions of W for the Ti-W alloy at different ratios of Ti and W from the direct simulations at respective temperatures T_m

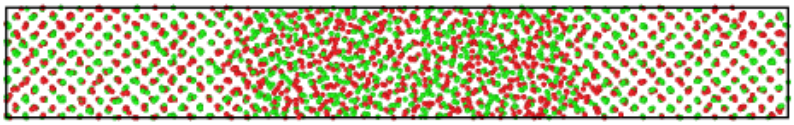

Figure 4.6: Frame 5500, ie 550 ps , of titanium-tungsten in a direct simulation with 50 percent Ti and 50 percent tungsten, it can be seen that the liquid and the solid phase both still exist. Thus the melting point could be reached. The system is visualized in OVITO.

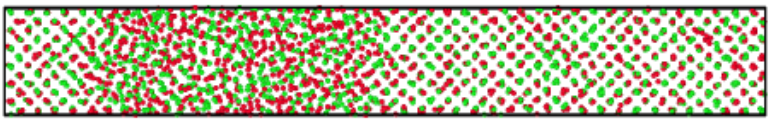

Figure 4.7: Frame 10000, ie 1 ns of titanium-tungsten in a direct simulation with 50 percent Ti and 50 percent tungsten, it can be seen that the liquid and the solid phase both still exist after another 550 ps in comparison to the time step after 450 ps . Thus the melting point could be reached. The system is visualized in OVITO.

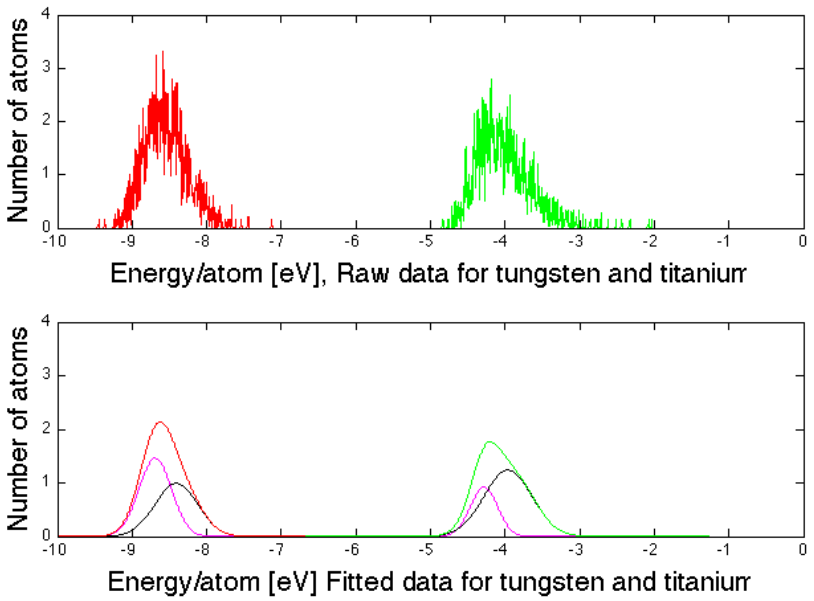

Figure 4.8: The raw data and fitted data for tungsten and titanium. The raw data of W is the red curve , the green curve is the titanium raw data.

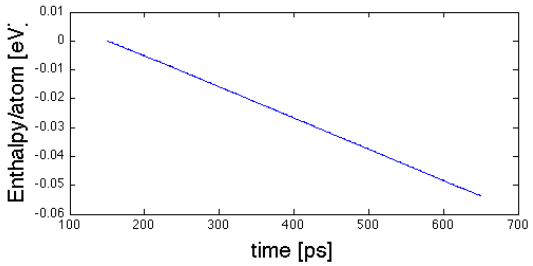

Figure 4.9: The enthalpy, in eV/atom, is plotted against the time, in ps. The enthalpy is the output from the NPH ensemble in LAMMPS from the production run.

In order to calculate the concentration and composition of the liquid and solid part in the alloy, Gaussian curves were fitted to the raw data. A fit for 0.5 Ti composition is shown in figure 4.8. The raw data of W is the red curve , the green curve is the Ti raw data. The fitted data has three curves, one each for W and Ti with a maximum around -8.5 $^{eV}/_{atom}$ and -4 $^{eV}/_{atom}$respectively. The two smaller curves represents the liquid distribution, which are the purple lines, and the solid distribution, which are the black lines for Ti and W. The larger curves are the actual fitting to the raw data of W and Ti.

To examine the credibility of the production run the variables of enthalpy, potential energy and temperature was analyzed The enthalpy in the NPH simulation should be constant, which is plotted in figure 4.9. It can be noted that the enthalpy for the 0.5 Ti simulation of 400 000 time steps was dropped by 0.087 $^{eV}/_{atom}$.

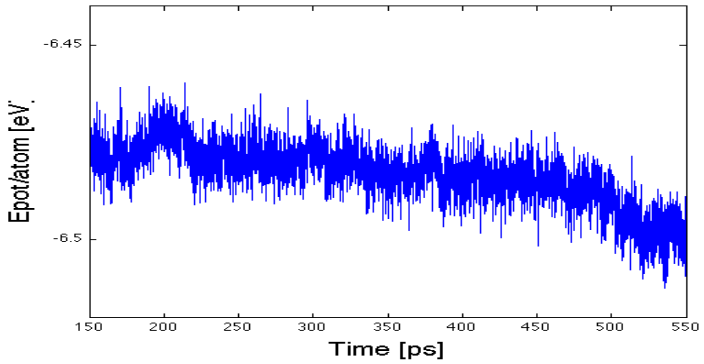

Figure 4.10: The raw data of the potential energy in eV plotted against time, in ps, in the NPH simulation

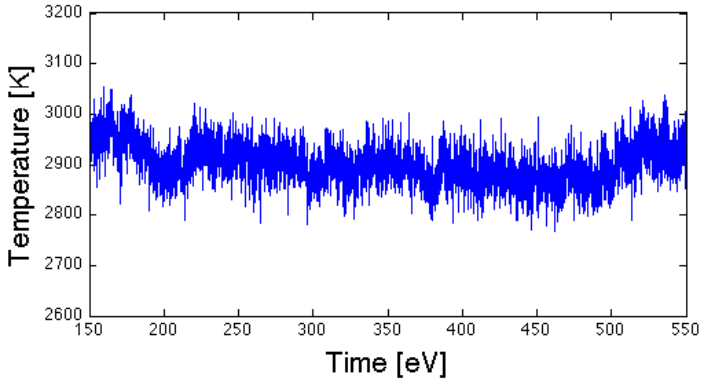

Figure 4.11: The raw data of the temperature in K plotted against time, in ps, from the production run.

The enthalpy of LAMMPS output from the NPH ensamble is the upper plot in figure 4.10. The enthalpy could be thought be the total energy as the pressure is set to zero, in LAMMPS however the NPH simulation has it's own PV term that is not the same as the other P and V identities that LAMMPS can give as output.

The potential energy, plotted in figure 4.10 appear to also drop after raising its potential energy in the NPH simulation with the same amount that the enthalpy did. Which could mean that the system hasn't yet reached equilibrium.

The temperature for the alloy with composition 0.5 Ti is plotted with respect to time in figure 4.11. The temperature appear to stabilize during the production run while the potential energy is dropping.

Analyzing Ti-W alloy in OVITO

The accuracy of the Gaussian fit to the raw data can be compared to handpicking the liquid and the solid atoms in OVITO and determining the phase diagram. By taking the mean of every 1000 time step in the NPH simulation from 3000 to 5500, an estimate of the accuracy of the Gaussian method is acquired. A comparison of

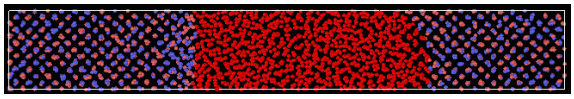

(a) This figure shows the selected liquid particles. The accuracy for one time frame could be better than the method of Gaussian fitting. The system is visualized in OVITO.

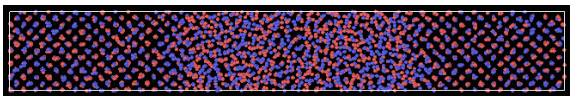

(b) The figure shows the system of a simulation of the W-Ti alloy in the production run, the liquid atoms can clearly be determined. The system is visualized in OVITO.

Figure 4.12: The figure illustrates the accuracy of hand picking liquid particles in OVITO.

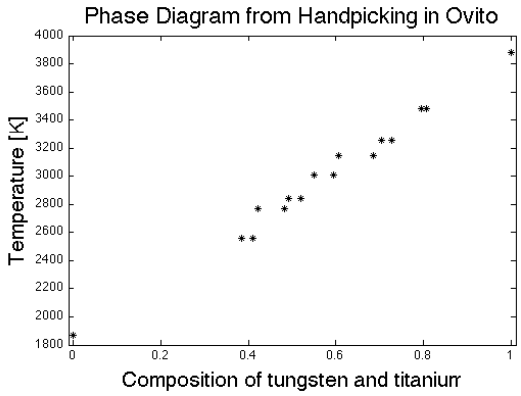

Figure 4.13: This figure shows an alternative method of retrieving the phase diagram, which is by handpicking the liquid atoms.

marked liquid atoms and non marked atoms are visualized with OVITO in figure 4.12

The phase diagram retrieved from this method generated the alloy phase diagram in figure 4.13. The first thing that could be noted is that the melting area appears to be smaller than the melting area Gaussian fitting generates.

4.2.4 High Temperature Phase Diagram

The result of all simulations with the direct method was the upper part of the phase diagram which is plotted in figure 4.14. The accuracy of the Gaussian fit to the raw data will have a crucial part in the upper part of the phase diagram.

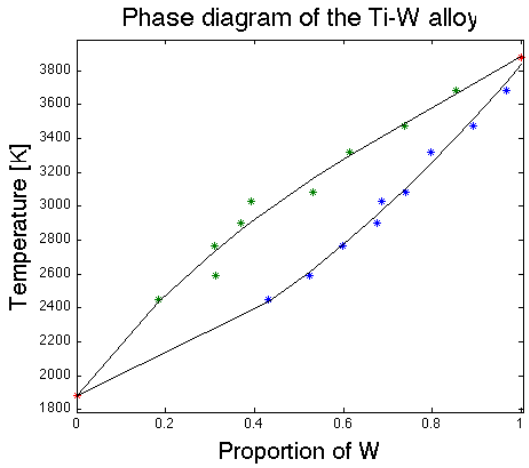

Figure 4.14: This is the melting line of the alloy titanium-tungsten.

4.3 Solid-Solid Transition

The results for the solid-solid transition will be presented starting with the information gathered from the ordinary MD-simulations. These simulation were mainly run in order to get good parameters for the λ-integration. Although other interesting features of the systems could also be obtained through these simulations

Following that, the results from the λ-integration will be shown and in the end of this chapter the low temperature phase diagrams will be given.

The goal from the beginning was to do use λ-integration to map out the phase diagram for the tungsten-titanium alloy. Unfortunately the λ-integration ultimately did not work to the extent that it could predict the phase transition in our system. Instead, the main focus for the lambda integration shifted to reproduce only the phase transition predicted in Tommy Andersson's thesis[2]. The phase diagrams are constructed with external enthalpy data provided by our supervisor Paul Erhart, see section 3.2.5, and common approximations for the entropy of mixing.

4.3.1 Pure Titanium and Tungsten

The first step for the lambda integration was to do a couple of pre-simulations in order to determine the enthalpy and the lattice parameter. The lattice parameter was important since the goal was to simulate in the NVT-ensemble while the enthalpy was needed for the Gibbs-Helmholtz equation. The corresponding plot of the enthalpy is shown in figure 4.15. An interesting feature of the enthalpy is the behavior around 1000 K, an indication that the system isn't entirely stable around this point could be noted.

The lattice parameter for titanium can be seen in table 4.4. Also, the thermal expansion for tungsten was illustrated in figure 4.16 as an example of another parameter that could be derived from MD-simulations alone. It is also an important

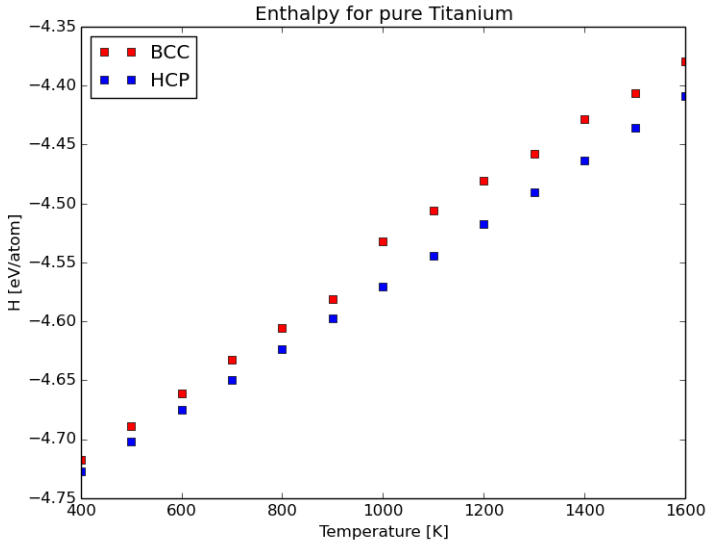

Figure 4.15: For this plot a pure titanium system was simulated in a NPT ensemble at different temperatures for both hcp and bcc structure. Notice the change around 1000 K which indicates an abrupt change in some property.

factor for eventual future studies of the titanium-tungsten system.

Following the NPT simulation which helped with the determination of the enthalpy and lattice parameter was the NVT simulation. This simulation helped to choose which spring constant to use.

The equation 3.4 predicts a spring constant of about 1.5 $^{eV}/_{Å}$ but as seen in figure 4.17 this was not as good as a value of about 3 $^{eV}/_{Å}$. Because of this, the spring constants for the integration steps were set to be around twice of the predicted value.

That was all the parameters needed to commence the actual integrations. Although first a series of test were needed to be performed in order to determine the simulation length.

Temp [K]	400	500	600	700	800	900	1000
bcc [Å]	3.278	3.283	3.290	3.296	3.299	3.300	3.314
hcp [Å]	2.925	2.929	2.933	2.936	2.940	2.944	2.947

(a) Lattice parameters for Titanium in the range 400 K to 1000 K

Temp [T]	1100	1200	1300	1400	1500	1600
bcc [Å]	3.317	3.319	3.322	3.324	3.326	3.328
hcp [Å]	2.951	2.954	2.957	2.960	2.963	2.966

(b) Lattice parameters for Titanium in the range 1100 K to 1600 K

Table 4.4: This is the lattice parameters for Titanium at different temperatures.

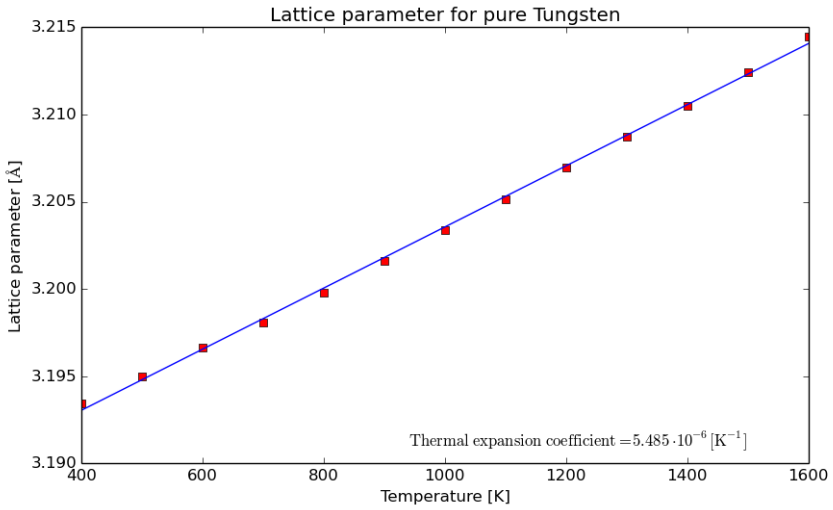

Figure 4.16: For this plot a pure tungsten system was equilibrated in a NPT ensemble for different temperatures. The lattice parameter for the bcc crystal was calculated for each temperature and used to compute the thermal expansion coefficient.

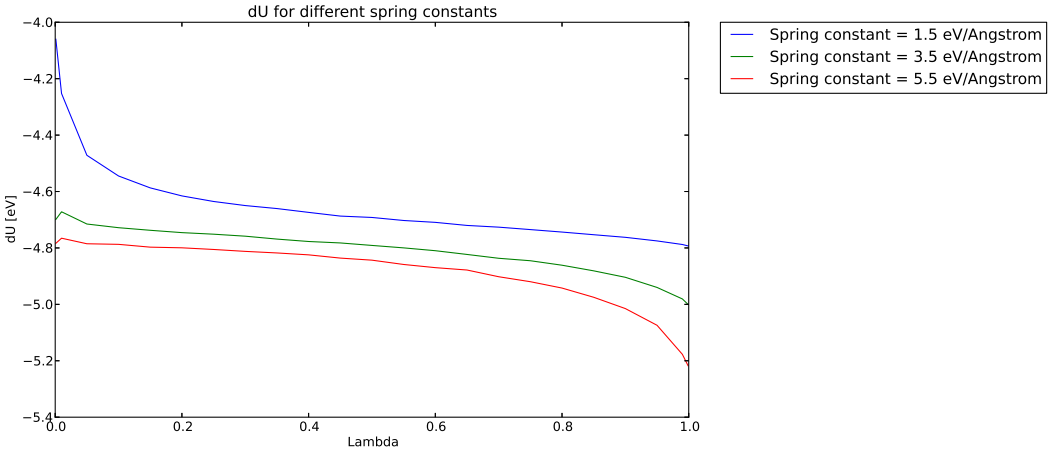

Figure 4.17: This is an illustration of how the spring constant affects the convergence. In theory the corresponding integral will converge to the change in energy but in practice one will get numeric errors for badly chosen spring constants. According to equation (3.4) a good guess would be 1.5 eV/Å but a larger value is apparently better.

First a convergence test was conducted for the single shot method to determine a good length of the simulation with respect to accuracy and time, the result can be seen in figure 4.18. A system of pure hcp titanium at 1200 K was simulated with 19 different switch times. The resulting values of the free energy was then compared to the value of a longer simulation of 200 ps. We are working with differences in the free energy in the order of 100 meV, so to be considered converged the absolute difference due to simulation length should be below 1 meV. We can se in the figure that convergence is reached after about 60 ps.

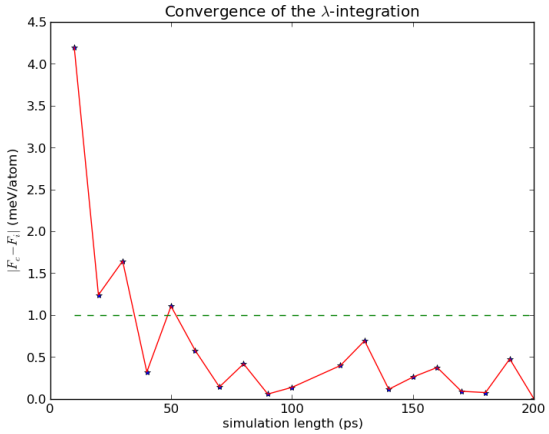

Figure 4.18: The figure illustrates the convergence of the single shot TDI method, that is the absolute difference in free energy between a long, well converged simulation and shorter simulations. We see that after about 60 ps the difference stays below1 meV, which should be sufficient for our needs. The system simulated is pure Ti in hcp at 1200 K.

An equivalent test was performed for the multi shot method which can be seen in figure 4.19. In this case a system of pure bcc Titanium were used instead. The test was performed for 20 different lengths between 10 ps and 200 ps and was compared to a run with 300 ps. The result is similar to the single shot method with a convergence of about 70 to 100 ps.

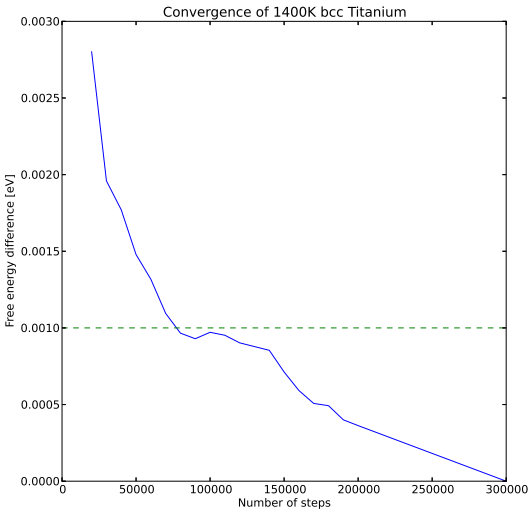

Figure 4.19: The figure illustrates the convergence of the multi shot TDI method, that is the absolute difference in free energy between a long, well converged simulation and shorter simulations. We see that after about 100 ps the difference stays below1 meV, which should be sufficient for our needs. The system simulated is pure Ti in bcc at 1400 K.

The hcp-bcc transition for pure titanium was calculated with the single shot

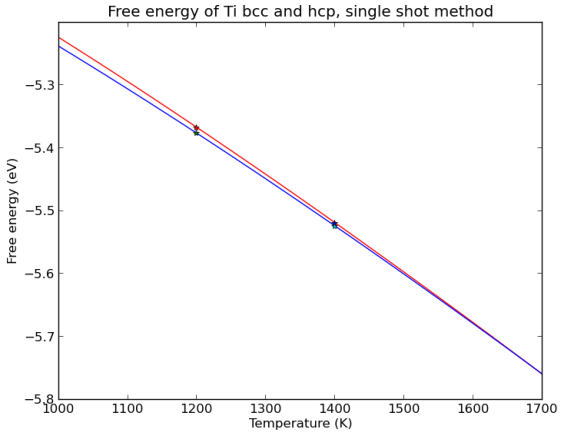

Figure 4.20: The figure shows the free energy of titanium calculated with the single shot method at different temperatures. Notice the cross of the lines at 1688 K, which indicate the transition temperature. The upper line is for bcc and the lower line is for hcp. The dots are the the TDI-data, while the interpolation and the extrapolation is done with GH curves from each TDI point that is then weighted together linearly with respect to which TDI point that is closest.

TDI method. The result can be viewed in figure 4.20. Notice the interception of the lines at 1688[K] , which indicates the transition temperature. As a reference, T. Andersson recieved a temperature of 1280 K with the same method [2]. Two points of free energy was simulated for each of the two phases, one at 1200[K] and one at 1400 K. The enthalpy was simulated at eight points evenly distributed between 1000 K and 1700 K for use in the GH formula. The free energy was extrapolated from each point using GH and then the resulting curves were weighted together linearly with respect to the distance from the respective TDI points.

The same transition was calculated with the multi shot TDI method and the result can be seen in figure 4.21. With this method we tried to replicate Tommy Anderssons results but couldn't find the transition at the expected value of 1280 K. The multi shot integration was performed for 100[ps] with a time step of 1 fs. The lambdas were evenly spaced between 0 and 1 in intervals of 0.05 steps except at the boundaries were also 0.001, 0.01, 0.99 and 0.999 were used to improve numeric accuracy. This choice is according to Andersson [2] a balance between accuracy and use of computational resources.

GH was also used but plotted from every point to indicate how accurat the data points are. A rough estimate is that the values are within 10 $^{\text{meV}}/_{\text{Å}}$.

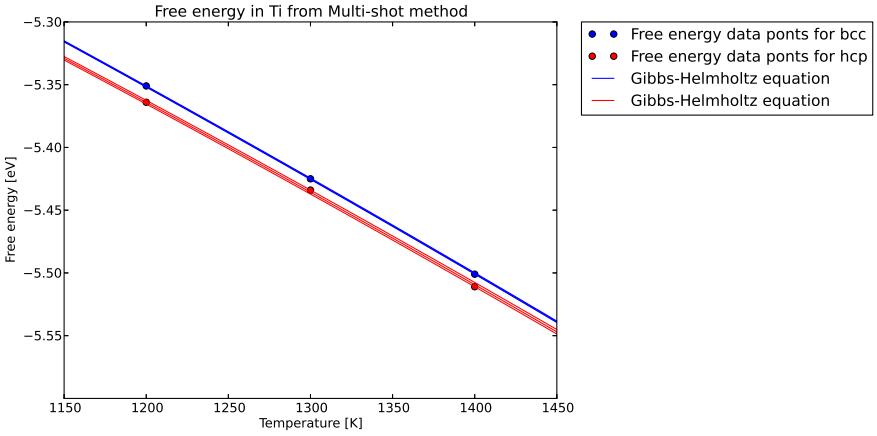

Figure 4.21

4.3.2 Mixtures of Titanium and Tungsten

For the mixtures two different phase diagrams were constructed. The first, shown in figure 4.22, was purely constructed from theoretical approximations. Outside the phase transition line an equilibrated system will only consist of one composition. However, inside the phase line an equilibrated system would be divided into two different compositions.

The second phase diagram is shown in figure 4.23. It was constructed from a combination of data provided by our supervisor [1] and a theoretical expression for S_{mix}.

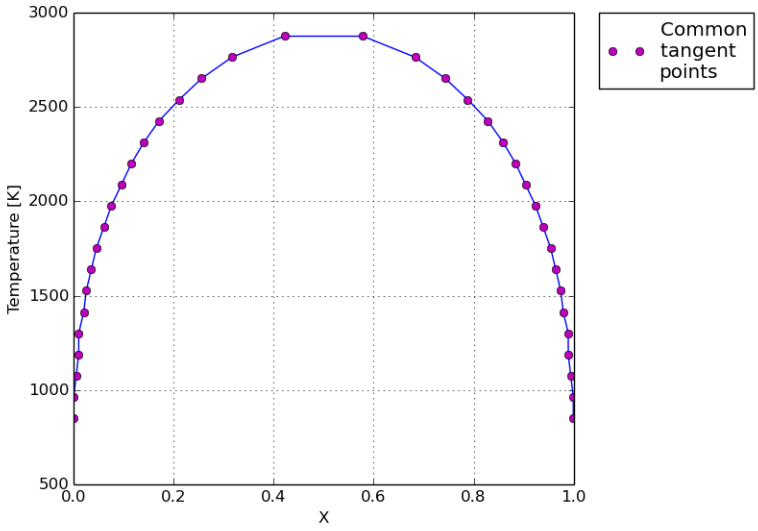

Figure 4.22: Phase diagram derived by using the entropy approximation seen in equation 2.11 and the expression in equation 3.6 with $\Omega = 1$ for the entropy of mixing. The common tangent points are found in figure 3.4 for several temperatures and then put together in this temperature-composition diagram.

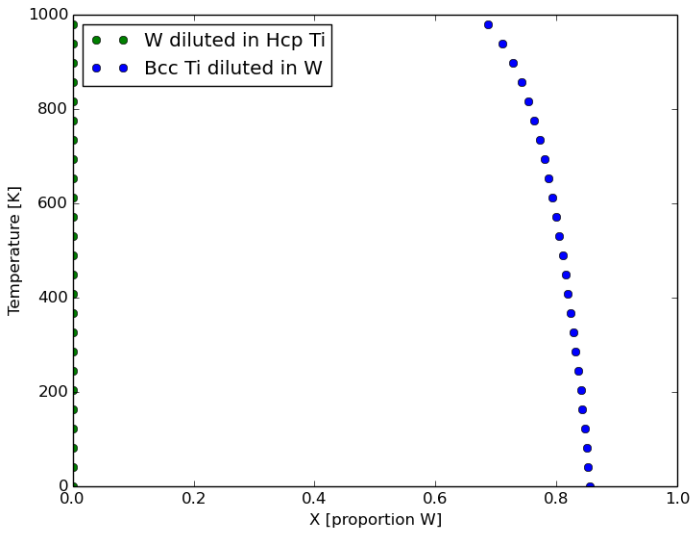

Figure 4.23: For this phase diagram data from simulations, see figure 3.5, was used for the H_{mix} part of the free energy and equation 2.11 was used for the S_{mix} part. For higher temperatures, the free energy of bcc Ti has to be considered for the right hand side of the diagram.

Chapter 5

Discussion

The simulations in LAMMPS that were conducted proved to be more complicated than expected. The result that is shown in figure 4.1 is partly consisting of results from our simulations and partly of analyzed data provided by our supervisor Paul Erhart[1].

The results from the λ-integration and the direct method will be discussed in section 5.1 and 5.2 respectively in greater details.

5.1 Liquid-Solid Transition

Our first approach to determine the melting lines was to use the NPT and NVE simulations. In order to check whether there were two phases left or not we planned to use a radial distribution function (RDF) and interpret the system qualitatively. The radial distribution is a histogram over the distances between all atom pairs and reflects the long and short range order of the system. The long range limit in the function looks different for a liquids and a solids, since a solid has long range order but a liquid has not. There were two problems with this approach. Firstly the NVE approach requires a good approximation of the melting temperature, which we didn't have access to because the determined melting interval was around 1000 K for the simulated system.

It would have been necessary to iterate through a large amount of initial energies with a small enough energy step to not miss the point. This would be a heavy computational task. This is regarded unsuitable and lead us on to the second problem. This is the possibility to check if the system has lost its two-phase coexistence, which is difficult to automate. Also our RDF approach proved to be insufficient for this task due to the fact that the RDF for the liquid and the solid are too similar.

We therefore changed our approach to keeping the enthalpy and pressure, instead of the energy, constant. In our new approach the change in energy was checked in each iteration. The method is more closely described under the method part of this report. This method is better at finding the melting point.

The direct method approach with NPT and NPH simulations produced results for the melting line. The melting point of Ti was determined to 1883 K with a standard deviation of 51 K. This is 58 K from the experimental value[12]. The melting point of W was determined to 3884 K with a standard deviation of 52 K this is 1185 K from the experimental value. The results from the alloy has a standard deviation from 37 dimension to 61 K. These standard deviations are about half the value of the standard deviation calculated in an article by Wu et al., 2011 [31] where they use the same software. The conclusion is that the results have quite low standard deviation. Therefore the statistical error is small, however, a systematic error can not be excluded for this reason.

The melting lines in between the melting point of Ti and W were determined with quite low accuracy. The Gaussian fit turned out to estimate a larger melting area than if the liquid and solid atoms were handpicked in OVITO. Consider figure 4.12a, the liquid atoms in the figure are the red atoms. These are selected to be liquid by hand. By comparing this to figure 4.12b where no atoms are picked, the accuracy for the distinction between the two phases is thought to be quite good.

The method of fitting Gaussian curves in order to determine concentrations of liquid Ti-W and solid Ti-W gave less accurate results. The problem was that MATLAB interprets the curves differently than desired and the result could be that the concentration is larger than 1 or smaller than 0 which is not possible physically. The reason is that the peaks for liquid and solid were not separated enough for MATLAB to resolve two accurate peaks. Another problem was that when MATLAB could make a fit as in figure 4.8 the uncertainty of the liquid and solid peaks is large due to low resolution.

The result obtained are depending on the potential used. The MEAM spline and CDIP potentials for the Ti, W and Ti-W system has not thoroughly been investigated for the melting line. The result should therefore not be dismissed based on the fact that the result are far from experimental results.

As the phases still remained after 1 ns and ratios of liquid and solid didn't change it should be reasonable to conclude that the melting point has been reached. The equilibrium with respect to the composition of the liquid and solid parts has however probably not been reached, this conclusion is made based on figure 4.10, where the potential energy seem to drop during the production run. Therefore the run time of the production run could have been chosen larger in order to reach equilibrium. Though this would cause the simulations to be very expensive as the simulations need to be iterated in the melting interval.

The system size 2956 atoms, or $(6x6x42)a$ where a is the lattice parameter, should be adequate, as no significant difference was seen in comparison to a system of 20 000 atoms. A system of 20 000 atoms has been used before in article from et al Wu, 2011 [31], with values that have the standard deviation in the magnitude of 100 K from experimental values.

The time step length effect LAMMPS:s accuracy as the Verlet algorithm must be solved. The time step was chosen to 1 fs, this was thought to be a reasonably small time step. Consider figure 4.9, in the figure the enthalpy is expected to remain constant. Because the enthalpy is dropping by 0.0870 eV/atom during the production run, comparing this to the initial value which was -6.086 eV makes the drop a 0.014 percent decline. A systematic error may therefore exist in the simulation. As a time step of 0.1 fs did not improve the decline in enthalpy nor a time step of 2 fs we ruled out that the enthalpy drop depended on the time step, which should have been the most likely reason for this error. Ultimately this problem could not be solved due to time limits.

5.2 Solid-Solid Transition

The goal from the beginning was to map out the complete phase diagram of the alloy in the solid region but unfortunately this could not be done. Even after a shift of focus to only simulate the solid phase transition between hcp and bcc Titanium the transition temperature could not be replicated from Andersson's thesis [2]. To aquire the lower part of the phase diagram we used data from our supervisor.

5.2.1 λ-integration

The overall conclusion regarding the λ-integration is that the method is powerful if used correctly, but that the method can be unstable and requires a great attention to detail in order to work well.

All of the pre-simulations went well and from that step alone a great deal of properties, for example the enthalpy and the lattice parameter, can be computed. Unfortunately, due to time limits, we couldn't compute the standard deviation for the sampled properties (the enthalpy, the lattice parameter and the free energy for the multi shot method). We did compute the standard deviation for titanium at 1400 K early in the project and the standard deviation didn't affect the GH extrapolation more than a couple of meV per atom. This shouldn't affect the accuracy very much but unfortunately we don't have data to support this claim.

Furthermore, things got complicated when the spring constant is to be chosen. Even though in theory, it should not matter which spring constant is chosen the numerics can go wrong when implementing it in practice. A good guess would be to choose the spring constant such that the Einstein crystal and the system has the same mean square displacement. According to our result the spring constant should be at least twice the predicted value in order to get good convergence in the numerics.

Another question that can be discussed is how sensitive the system is to changes in the lattice parameter. By the calculations in this report, we only know that the lattice parameter changes with increasing temperature, but no further analysis is

done. It could be that even a minimal change in the lattice parameter increases the pressure so much that it could no longer be approximated to zero.

The test of convergence indicated that the length of the simulation should be enough and the spring constant was not off by miles. The extrapolation with Gibbs Helmholtz also indicates that the free energy values are converged. This arises suspicions that there is some kind of systematic error.

5.2.2 Phase Diagrams

Using simulations many predictions of a phase diagram can be made. Figure 4.22 illustrates how the importance of the entropy term in the free energy raises with temperature. The system will become more disordered for higher temperatures. The enthalpy expression that is used for this phase diagram, equation 3.6, is always positive. This means the enthalpy term of the free energy will make it more favorable for the system not to mix. However, as this term is independent of temperature its importance decreases for higher temperatures.

The enthalpy curves shown in figure 3.5 has both positive and negative values. Positive values exists for the hcp titanium rich part. This indicates that tungsten has rather low solubility in hcp Ti. In the corresponding phase diagram, figure 4.23, this translates to a straight line on the left hand side. Negative values exist for the bcc tungsten rich part. This indicates that Ti has some solubility in bcc W. The effects of this can be seen in the lower right part of the phase diagram.

For these phase diagrams only H_{mix}, and not the total enthalpy of the simulated system, is considered. The difference $H_{vib} = H_{tot} - H_{mix}$ is a straight line between the enthalpy of the pure substances and will not affect the common tangent construction. As the values for H_{vib} are about 100 times larger than H_{mix} it can be numerically difficult to get good polynomial fits of the data without first removing H_{vib}. The value of H_{vib} for a mixture corresponds to the total enthalpy of a system with the same amount of both elements as the mixture, only without any interaction between the elements.

It is important to keep in mind that even though the data for H_{mix} is independent of temperature, it is not accurate for all temperatures. For the Ti rich part, the bcc structure will become lower in free energy than the hcp structure for some temperature. Exactly at what temperature this happens depends on the composition but for pure titanium Tommy Andersson computed it to be 1280 K [2]. As his simulations were similar to ours, this transition temperature is of greater relevance than the experimental one. Close to, and above this temperature a common tangent construction between a bcc Ti rich system, and the already considered hcp Ti rich and bcc W rich systems might be possible. This would affect the outcome of the phase diagram. As indicated by the steep incline of the fitted line in figure 3.5 and the fact that pure W does not exist in a hcp structure [15], hcp W rich systems does not have to be considered. This is the reason for using a straight line for the data

fitting of this region.

Chapter 6

Conclusion and Outlook

In conclusion the direct simulations of the melting lines could be determined with quite low statistical error, which are visualized in figure 4.14. The method itself is considered to be a stable method which is used often and therefore the melting points of pure W and Ti can be considered quite accurate. However the method of determining the melting lines of the alloy turned out not to be a adequate method due to low resolution of the potential energy per atom. The low resolution can be seen in figure 4.8.

Further conclusion is that the temperature appear to equilibrate but the potential energy and the enthalpy are dropping in the production run which is an indication of not reaching the equilibrium with respect to composition, but also that the simulation is not physical.

The lambda integration is also a common method and although computationally expensive it can be quite powerful. The method has been proved to work on our system by Tommy Andersson [2] but we couldn't replicate the results from his work. We suspect that the problem is some kind of systematic error. The method is quite complex with a lot of parameters that need to be carefully determined. The pre simulations went well and a lot of information can be determined from those simulations alone. In our case the enthalpy and lattice parameter were computed.

MD-simulation in general is a powerful method and widely used. Unfortunately the methods used are quite delicate and the parameters for the simulations must be carefully chosen. Not only can the method predict properties of materials but combined with statistical mechanics, a great feel and understanding can be gained about the world around us.

For future reference and projects a python code would probably be suitable for determining the composition of the liquid and solid when determining the melting lines. This would give the melting lines higher accuracy if written correctly.

The λ-integration could benefit from more thorough studies about how errors in the enthalpy and lattice parameter affects the accuracy of the calculated free energy.

Bibliography

[1] Erhart, P. (2014) Private communication.

[2] Andersson, T. (2012) *One-shot free energy calculations for crystalline materials.* Göteborg : Chalmers University of Technology

[3] Murray, J.L. (1981) *The Ti-W (Titanium-Tungsten) System.*

[4] Tungsten Titanium Alloy (2014) *American Elements* `http://www.americanelements.com/wtia.html` (10 Feb. 2014).

[5] Klueh, R.L. (1990) *Reduced Activation Materials for Fusion Reactors.* 1047th edition. ASTM International.

[6] Lee, S.K., Lee, Nyung Lee (1986) Calculation of Phase Diagrams using Partial Phase Diagram Data. Calphad, Vol.10, No.1, pp. 61-76.

[7] Porter, D.A., Easterling, K.A. (1992) *Phase Transformations in Metals and Alloys.* 2nd Edition. London: Chapman & Hall.

[8] C. Nordling, J. Österman. (2006) *Physics Handbook.* Edition 8:4. Lund: Studentlitteradtur AB.

[9] Schroeder, D. (2000) *An Introduction to Thermal Physics.* Addison Wesley Longman.

[10] Frenkel, D., Smit, B. (2002) *Understanding Molecular Simulations: From Algorithms to Applications.* 2nd Edition. Academic Press.

[11] *Gibbs–Helmholtz ekvation.* `http://www.ne.se/gibbs-helmholtz-ekvation`, Nationalencyklopedin, [Accessed 2014-05-19].

[12] Donachie, M.J. (2000) *Titanium: A Technical Guide.* ASM International.

[13] [HCP crystal structure] 2013 [image online] Available at: <`http://scioly.org/wiki/index.php/File:Hcp.gif`> [Accessed 2014-02-10].

[14] [BCC crystal structure] 2006 [image online] Available at: <http://en.wikipedia.org/wiki/File:Lattice_body_centered_cubic.svg> [Accessed 2014-02-10].

[15] Lassner, E., Schubert, W.D. (1999) *Tungsten: Properties, Chemistry, Technology of the Elements, Alloys, and Chemical Compounds*. New York: Springer

[16] [Phase diagram for Titanium] n.d. [image online] Available at: <https://dtrinkle.matse.illinois.edu/research:ti> [Accessed 2014-02-10].

[17] [Phase diagram for Tungsten] 1975 [image online] Available at: <http://commons.wikimedia.org/wiki/File:Phase_diagram_of_tungsten_(1975).png> [Accessed 2014-02-10].

[18] Bransden, B., Joachain, C. (2003) *Physics of atoms and molecules*. 2nd Edition. Harlow: Pearson Education Limited.

[19] *pair_style meam command.* (2014) http://lammps.sandia.gov/doc/pair_meam.html (2014-05-15)

[20] Sadigh B., Erhart P., Stukowski A., Caro A. (2009) *Composition-dependent interatomic potentials: A systematic approach to modelling multicomponent alloys.* In press. Philosophical Magazine A, Vol.89.

[21] Wang, L., van de Walle, A. (1012) Ab initio calculations of the melting temperatures of refractory bcc metals. Chemical Physics Letters, Vol.14.

[22] Wang, J., Yoo, S., Bai, J., Morris, J., Zeng, X. (2005) Melting temperature of ice Ih calculated from coexisting solid-liquid phases. The journal of Chemical Physics, Vol.123, pp. 1529-1534.

[23] Kirkwood, J. G. (1935) *Statistical mechnics of fluid mixtures.* The Journal of Chemical Physics. 3, 300-313.

[24] Frenkel, D. & Ladd, A. J. C. (1984) *New Monte Carlo method to compute the free energy of arbitrary solids. Application to the fcc and hcp phases of hard spheres.* The Journal of Chemical Physics. 81, 3188–3193.

[25] Plimpton, S. (1995) *Fast Parallel Algorithms for Short-Range Molecular Dynamics.* J Comp Phys. 117. http://lammps.sandia.gov

[26] Chalmers centre for scientific and technical computing at Chalmers University of Technology in Gothenburg Sweden (2014) C3SE. http://www.c3se.chalmers.se/index.php/Main_Page. (2014-05-19).

[27] Park H., Lenosky T. Unpublished.

[28] Hennig R., Lenosky T., Trinkle D., Rudin S., Wilkins J. (2008) *Classical potential describes martensitic phase transformations between the α, β and ω titanium phases.* Physical review. B 78.

[29] Erhart P., Stukowski A. Unpublished.

[30] Stukowski, A. (2010) *Visualization and analysis of atomistic simulation data with OVITO - the Open Visualization Tool.* Modelling Simul. Mater. Sci. Eng. 18.

[31] Wu, Y., Wang, L., Huang, Y., Wang, D. (2011) Melting of copper under high pressures by molecular dynamics simulation. Chemical Physics Letters, Vol.515, pp. 217-220.

[32] *Fix ti/spring command.* (2014) `http://lammps.sandia.gov/doc/fix_ti_spring.html`. [Accessed 2014-05-19].

Appendix A

LAMMPS

This is an example of LAMMPS code and parts of the output from a terminal

A.1 code

```
# Basic initialization
dimension  3
boundary p p p
units metal
atom_style atomic

# Defining lattice, regions and creating the atoms
lattice fcc 3.61
#lattice bcc 2.95 (Ti)

variable side equal 6
variable s1 equal ${side}/2.0
variable s2 equal ${side}/2.0+1

region simulationBox block 0 ${side} 0 ${side} 0 ${side}
region liquidBox block 0 ${s1} 0 ${side} 0 ${side}
region solidBox block ${s2} ${side} 0 ${side} 0 ${side}

create_box 1 simulationBox
create_atoms 1 region liquidBox
create_atoms 1 region solidBox

group liquid region liquidBox
group solid region solidBox
```

```
# Defining the properties of the atoms
mass 1 63.55
#mass 1 79.87 (Ti)

pair_style eam
pair_coeff 1 1 Cu_u3.eam

neighbor 0.3 bin
neigh_modify every 20 delay 0 check no

# Setting the temperature
variable TStartLiquid equal 5000
variable TStartSolid equal 100
variable TExpected equal 1084

#variable TStartLiquid equal 5000 (Ti)
#variable TStartSolid equal 1000 (Ti)
#variable TExpected equal 1941 (Ti)

velocity liquid create ${TStartLiquid} 87287
velocity solid create ${TStartSolid} 87287

# Pre-running to initiate the system to the approximate temperature


# Fixes for the actual simulation
fix myFix all nve

# Dumping, logging and such
dump myDump all custom 200 dump/shouldWork.*.dump id xu yu zu

thermo_style custom step temp etotal pe press pxx pyy pzz vol
thermo 1000

# Timestep and run
run 20000
```

A.2 Terminal output

This is how a common terminal output from LAMMPS look like. Notice that it's not from the code above.

```
LAMMPS (16 Sep 2012)
Lattice spacing in x,y,z = 3.31922 3.31922 3.31922
Created orthogonal box = (0 0 0) to (19.9153 19.9153 19.9153)
  2 by 2 by 4 MPI processor grid
Created 432 atoms
Setting atom values ...
  432 settings made for type/fraction
CDIP linearized_mode=0
CDIP legacy_mode=0
CDIP ntypes=2
CDIP sigma_cutoff=5.5
CDIP sigma_stepsize=0.0276382
CDIP nknots=200
CDIP pair_pot_cutoff=5.5
CDIP pair_pot_stepsize=0.0276382
CDIP nknots=200
Setting up run ...
Memory usage per processor = 4.95452 Mbytes
Step Temp Enthalpy Lx PotEng varPotEC
       0         2400   -4.6862658    19.915314   -4.7099566            0
     100      55.7722   -3.0546794    19.915314   -3.5877417   0.29029315
     200    2102.9502   -4.4258603    19.915314    -4.669579  0.028296539
     300    468.23415   -3.5895698    19.915314   -3.9464079   0.22898296
     400    1464.9511   -4.1093414    19.915314   -4.4654485   0.10217556
     500    1155.3086   -3.9610809    19.915314   -4.3463666    0.1416101
     600    739.46849   -3.7373785    19.915314   -4.0996492   0.19156364
     700     1852.027   -4.3091982    19.915314   -4.6177202  0.055998711
     800    187.58086   -3.2131493    19.915314    -3.704991   0.26164326
     900    2269.6709   -4.6556404    19.915314   -4.7058194 0.0054898805
    1000    4.3449743   -3.1311935    19.915314   -3.6172278   0.28560625
    1100    2227.6075   -4.5757466    19.915314   -4.6937385  0.010523563
    1200    257.05319    -3.343278    19.915314   -3.8017536   0.25400247
    1300    1744.3203   -4.2329071    19.915314   -4.5522024  0.069114816
    1400    864.66531   -3.9237741    19.915314   -4.2136737   0.17860842
    1500    1031.2524   -3.6744302    19.915314   -4.1783864   0.15732695
    1600    1602.2625   -4.1886939    19.915314   -4.5401414  0.088737225
```